

1 Aerosol emissions from prescribed fires in the United States:  
2 A synthesis of laboratory and aircraft measurements

3

4 A. A. May<sup>1%</sup>, G. R. McMeeking<sup>1#</sup>, T. Lee<sup>1\$</sup>, J. W. Taylor<sup>2</sup>, J. S. Craven<sup>3</sup>, I. Burling<sup>4@</sup>, A. P. Sullivan<sup>1</sup>, S.  
5 Akagi<sup>4</sup>, J. L. Collett, Jr.<sup>1</sup>, M. Flynn<sup>2</sup>, H. Coe<sup>2</sup>, S. P. Urbanski<sup>5</sup>, J. H. Seinfeld<sup>3</sup>, R. J. Yokelson<sup>4</sup>, and S. M.  
6 Kreidenweis<sup>1\*</sup>

7

8 <sup>1</sup>Department of Atmospheric Science, Colorado State University, Fort Collins, Colorado, USA

9 <sup>2</sup>Centre for Atmospheric Science, University of Manchester, Manchester, United Kingdom

10 <sup>3</sup>Division of Chemistry and Chemical Engineering, California Institute of Technology, Pasadena,  
11 California, USA

12 <sup>4</sup>Department of Chemistry, University of Montana, Missoula, Montana, USA

13 <sup>5</sup>Fire Sciences Laboratory, United States Forest Service, Missoula, Montana, USA

14 #Now with Droplet Measurement Technologies, Inc., Boulder, CO

15 %Now with Department of Civil, Environmental, and Geodetic Engineering, The Ohio State University,  
16 Columbus, Ohio, USA

17 \$Now with Department of Environmental Science, Hankuk University of Foreign Studies, Seoul, Korea

18 @Now with Cytec Canada, Niagara Falls, Ontario, Canada

19 \*Contact author: sonia@atmos.colostate.edu

20

21 **Abstract**

22 Aerosol emissions from prescribed fires can affect air quality on regional scales. Accurate representation  
23 of these emissions in models requires information regarding the amount and composition of the emitted  
24 species. We measured a suite of sub-micron particulate matter species in young plumes emitted from  
25 prescribed fires (chaparral and montane ecosystems in California; coastal plain ecosystem in South  
26 Carolina), as well as from open burning of over 15 individual plant species in the laboratory. We report  
27 emission ratios and emission factors for refractory black carbon (rBC) and sub-micron non-refractory  
28 aerosol and compare field and laboratory measurements to assess the representativeness of our laboratory-  
29 measured emissions. Laboratory measurements of organic aerosol (OA) emission factors for some fires  
30 were an order of magnitude higher than those derived from any of our aircraft observations; these are  
31 likely due to high fuel moisture contents, lower modified combustion efficiencies and less dilution  
32 compared to field studies. Non-refractory inorganic aerosol emissions depended more strongly on fuel

33 type and fuel composition than on combustion conditions. Laboratory and field measurements for rBC  
34 were in good agreement when differences in modified combustion efficiency were considered; however,  
35 rBC emission factors measured both from aircraft and in the laboratory during the present study using the  
36 Single Particle Soot Photometer were generally higher than values previously reported in the literature,  
37 which have been based largely on filter measurements. Although natural variability may account for some  
38 of these differences, an increase in the BC emission factors incorporated within emission inventories may  
39 be required, pending additional field measurements for a wider variety of fires.

## 40 1. Introduction

41 Prescribed fires are open biomass burning (BB) activities that may result in negative anthropogenic  
42 impacts on local-to-regional air quality and climate. Despite its potential drawbacks, prescribed fire is  
43 often the best option for maintaining and restoring native, fire-adapted ecosystems [*Carter and Foster*,  
44 2004]. Conversely, fire suppression and/or the absence of prescribed fire can increase fuel loads above  
45 natural levels and potentially increase the likelihood of extreme wildfires [*Fernandes and Botelho*, 2003;  
46 *Flannigan et al.*, 2009] and their associated negative impacts on ecosystems [*Miller et al.*, 2008], climate  
47 [*Westerling et al.*, 2006] and air quality [*Spracklen et al.*, 2009]. Particulate emissions from prescribed  
48 fires play a major role in determining their atmospheric impacts. Smoke from wildfires and prescribed  
49 fires has been shown to increase particulate matter (PM) concentrations in urban areas [*Phuleria et al.*,  
50 2005; *Hu et al.*, 2008; *Liu et al.*, 2009] and degrade visibility on regional scales [*McMeeking et al.*, 2006;  
51 *Park et al.*, 2007].

52 The major PM species emitted from fires are primary organic aerosol (OA) and black carbon  
53 (BC), though inorganic components such as nitrate ( $\text{NO}_3^-$ ), sulfate ( $\text{SO}_4^{2-}$ ), ammonium ( $\text{NH}_4^+$ ), chloride  
54 (denoted as  $\text{Cl}^-$ , per the Aerodyne Aerosol Mass Spectrometer community nomenclature), potassium  
55 ( $\text{K}^+$ ), and sodium ( $\text{Na}^+$ ) can be important depending on the fire/fuel type [*Reid et al.*, 2005; *Hosseini et*  
56 *al.*, 2013]. The open burning of biomass (e.g., forests, fields, savannas, and urban/rural waste, but

57 excluding cooking fires and biofuels) generates approximately 40% of the mass of globally-averaged  
58 annual sub-micron BC aerosol emissions and 65% of primary sub-micron organic carbon (OC) emissions  
59 [Bond *et al.*, 2013]. BC absorbs light over a broad range of wavelengths, and its presence in the  
60 atmosphere has significant effects on the radiative balance of the atmosphere, snow and ice albedo, and  
61 visibility [Ramanathan and Carmichael, 2008; Bond *et al.*, 2013]. Organic aerosol primarily scatters  
62 light, but some components emitted by fires have been shown to also absorb light strongly at near-UV  
63 wavelengths [Kirchstetter *et al.*, 2004; Andreae and Gelencsér, 2006; Lewis *et al.*, 2008; Magi, 2009;  
64 Lack *et al.*, 2012; Saleh *et al.*, 2013]. Chemical transport models used to predict regional air quality and  
65 global climate impacts require accurate BC emission inventories to correctly simulate column BC loading  
66 and absorption aerosol optical depth [Koch *et al.*, 2009]. These models also require accurate estimates of  
67 OA emissions as well as an appropriate treatment for the partitioning of semi-volatile species and for  
68 secondary production of additional OA from oxidation of primary emissions [Robinson *et al.*, 2007, 2010;  
69 Grieshop *et al.*, 2009b; Hennigan *et al.*, 2011; May *et al.*, 2013; Ortega *et al.*, 2013].

70 Two approaches are commonly used to create emission inventories for BB: "bottom up", in which  
71 total emissions are calculated by multiplying the mass of biomass consumed by an emission factor (EF, g  
72 species emitted per kg fuel burned), and "top down", in which the emissions are inferred from the amount  
73 required to reproduce the observed loading in the atmosphere, accounting for other sources. Major  
74 uncertainties for either approach are that fires and their emissions can be difficult to detect via satellite  
75 [Wiedinmyer *et al.*, 2006, 2011; van der Werf *et al.*, 2010] due to clouds, orbital gaps, sensitivity, and  
76 other problems [Giglio *et al.*, 2013], that BB emissions have not been fully characterized (i.e., not all  
77 emitted compounds have been identified) [Yokelson *et al.*, 2013a], and that the processes affecting  
78 atmospheric physicochemical aging of BB emissions are not completely understood [Jimenez *et al.*, 2009;  
79 Akagi *et al.*, 2012; Heilman *et al.*, 2014].

80 Emission factors for BB have been measured in the laboratory, from aircraft, and on the ground  
81 for many years, and have been compiled elsewhere [Andreae and Merlet, 2001; Akagi *et al.*, 2011]. Many  
82 previous biomass burning BC and OA emission measurements used filter-based light absorption [e.g.,

83 *Paris et al.*, 2009] or thermal-optical analysis [e.g., *Formenti et al.*, 2003] to quantify emissions from  
84 fires. However, these measurement techniques often disagree, by factors as large as four, even for the  
85 same filters when analyzed via different protocols [*Watson et al.*, 2005; *McMeeking et al.*, 2009]. Further,  
86 different approaches yield different operationally-defined carbonaceous aerosol, although the terminology  
87 has been inappropriately substituted in the literature; light absorption provides measurements of BC,  
88 while thermal-optical analysis provides measurements of elemental carbon (EC).

89 Both approaches have associated complications. The presence of light-absorbing organic material  
90 frequently found in BB emissions impacts filter-based approaches because the light-absorbing organic  
91 material can be erroneously interpreted as BC [*Kirchstetter et al.*, 2004], or the organic material biases the  
92 absorption measurement itself due to coating effects [*Subramanian et al.*, 2007; *Cappa et al.*, 2008; *Lack*  
93 *et al.*, 2008]. Thermal-optical analyses may differ due to various factors (e.g., instrument model, analysis  
94 protocol), which may affect the charring of organic carbon (OC) and OC/EC split [e.g., *Yu et al.*, 2002;  
95 *Chow et al.*, 2004, 2007]. Further, filter-based measurements typically cannot provide any information  
96 regarding the particle size distribution of uncoated BC “cores”, which, together with its mixing state, will  
97 affect the atmospheric lifetime and aerosol optical properties of the BC particles [*Bond and Bergstrom*,  
98 2006; *Lack and Cappa*, 2010; *Lack et al.*, 2012; *Bond et al.*, 2013].

99 The development of highly-sensitive, continuous or semi-continuous instruments such as the  
100 Droplet Measurement Technologies (DMT) Single Particle Soot Photometer (SP2) and Aerodyne Aerosol  
101 Mass Spectrometer (AMS) has provided the ability to measure refractory BC (rBC) mass concentrations  
102 and non-refractory sub-micron particulate mass concentrations (including OA), respectively, in the  
103 absence of a filter medium, avoiding many artifacts associated with filter sampling. The SP2 provides a  
104 different measure of BC compared to absorption measurements by quantifying the refractory material in  
105 the absorbing aerosol [*Slowik et al.*, 2007; *McMeeking et al.*, 2010; *Liu et al.*, 2011; *Petzold et al.*, 2013],  
106 whereas BC mass concentrations estimated using absorption methods are sensitive to the presence of  
107 coatings and/or organic species affecting light absorption [*Subramanian et al.*, 2007; *Cappa et al.*, 2008;  
108 *Lack et al.*, 2008]. Hence, we use “rBC” to refer to the operationally-defined measurements from the SP2,

109 while “BC” refers to estimates made using any light absorption technique. There have been few  
110 comparisons between rBC mass concentrations measured by the SP2 and BC mass concentrations  
111 measured by the thermal-optical methods on which many BB emission estimates are based [e.g., *Andreae*  
112 *and Merlet*, 2001]. Several studies have compared BC measured by several different techniques,  
113 including thermal-optical analysis and the SP2 [e.g., *Slowik et al.*, 2007; *Kondo et al.*, 2011a; *Yelverton et*  
114 *al.*, 2014], but did not examine biomass burning samples directly, so it is unclear how to infer how well  
115 BB emission factors from the filter-based approach and SP2 compare. Thus, the poor constraints on BC  
116 emission factors arising from previous measurement methods and limited observations remain a  
117 significant source of uncertainty in emission estimates [e.g., *Bond et al.*, 2013]. It is therefore of interest  
118 to measure rBC emission factors from BB using the SP2 for comparison with earlier estimates.

119         The SP2 has been previously used to measure rBC concentrations and physical properties in the  
120 atmosphere, including some sampling of biomass burning emissions [*Schwarz et al.*, 2008; *Spackman et*  
121 *al.*, 2008; *Kondo et al.*, 2011b; *Sahu et al.*, 2012; *Dahlkötter et al.*, 2014]. *Spackman et al.* [2008]  
122 reported rBC emission ratios (ER) to excess carbon monoxide (CO) for a biomass burning plume  
123 encountered over Texas that were 25-75% higher than those recommended for EC by *Andreae and Merlet*  
124 [2001] for extratropical fires and speculated that some of the differences may be due to variations in fuel  
125 burned although combustion efficiency plays the major role. Conversely, the ER observed by both *Kondo*  
126 *et al.* [2011b] and *Sahu et al.* [2012] were less than the values from *Andreae and Merlet* [2001]. This  
127 demonstrates that there is substantial variability in the BC emissions from BB, and hence, there is clearly  
128 a need for additional measurements of BC emission factors.

129         Similarly, the AMS has been used to measure non-refractory aerosol emissions from fires in  
130 several recent field campaigns focusing on biomass burning emissions [*Capes et al.*, 2008; *DeCarlo et al.*,  
131 2008; *Cubison et al.*, 2011; *Hecobian et al.*, 2011; *Akagi et al.*, 2012; *Jolleys et al.*, 2012]. Emission ratios  
132 of OA from these studies agree within roughly a factor of two compared to compiled BB emission  
133 inventories [*Andreae and Merlet*, 2001; *Akagi et al.*, 2011], although there may be substantial natural  
134 variability (i.e., the range of ER in the literature spans roughly one order of magnitude). To our

135 knowledge, only one recent study [Akagi *et al.*, 2012] has examined online PM emissions from prescribed  
136 fires in the US at the source via airborne sampling using both SP2 and AMS; however, this work focused  
137 mainly on transformations of OA (e.g., physicochemical aging) for a single plume. Here, we describe a  
138 new set of measurements of rBC and non-refractory PM in emissions from prescribed fires in the US,  
139 including well-characterized laboratory fires and aircraft measurements in young plumes from prescribed  
140 fires in California and South Carolina. Our goals are to examine the relationships between aerosol  
141 emissions and plant species, ecosystem, and fire combustion conditions in order to provide a reference set  
142 of EF and ER measurements for use in emission inventories for North American prescribed fires, and to  
143 examine reasons for any discrepancies between laboratory- and aircraft-measured emissions. Here, we  
144 only present fire-averaged EF and ER, rather than investigating emissions during fire phases (e.g.,  
145 flaming versus smoldering), as the average values are what are included in most emissions inventories  
146 [van der Werf *et al.*, 2010; Wiedinmyer *et al.*, 2011] and nearly all global chemical transport models that  
147 are used to predict atmospheric impacts of wildfires. Additionally, we provide mass-equivalent particle  
148 diameters of uncoated rBC present in the emissions from these fires as these values can assist in  
149 predictions of aerosol radiative forcing in global climate models as well as size-resolved aerosol chemical  
150 composition in chemical transport models.

## 151 **2. Experiment details**

152 We present results from a laboratory-based campaign in 2009 and aircraft campaigns in 2009 and 2011.  
153 The laboratory campaign took place at the United States (US) Forest Service Fire Sciences Laboratory  
154 (FSL) in Missoula, Montana during the third Fire Laboratory At Missoula Experiment (FLAME-III). It  
155 was the third of a series of related, but independent, experiments at the FSL examining the properties of  
156 fire emissions. The aircraft campaigns focused on measuring emissions from prescribed fires over  
157 California (San Luis Obispo Biomass Burning Experiment; SLOBB) and South Carolina (South Carolina  
158 fiRe Emissions and Aging Measurements; SCREAM) in the US, summarized in Table 1. Each campaign

159 featured extensive trace gas and aerosol instrumentation, but we only describe instruments directly  
160 relevant to the analysis presented in the following sections. Additional information regarding other  
161 measurements and experiments performed during these campaigns can be found elsewhere [*Burling et al.*,  
162 2011; *Hennigan et al.*, 2011, 2012; *Akagi et al.*, 2012, 2013, 2014; *Engelhart et al.*, 2012; *May et al.*,  
163 2013; *Ortega et al.*, 2013; *Sullivan et al.*, 2014].

## 164 **2.1 Facilities, fuels and site descriptions**

165 The FSL features an approximately 3000 m<sup>3</sup> combustion chamber suitable for the measurement of gas  
166 and particle emissions from laboratory fires on timescales of several hours [*Christian et al.*, 2003;  
167 *McMeeking et al.*, 2009]. We conducted 27 burns, in which smoke emissions from the ignited biomass  
168 filled the sealed yet not airtight combustion chamber and were sampled by instruments located in adjacent  
169 laboratories to characterize primary emissions with no photochemical aging. Each burn experiment lasted  
170 approximately three hours. Smoke was actively mixed within the room by a large fan located on the floor.  
171 The emissions were fire-integrated for the duration of the experiment after the room had become well-  
172 mixed (since the smoke was retained within the combustion chamber) to remove potential initial biases  
173 since gases diffuse faster than particles.

174 Plant species burned during FLAME-III were mostly those commonly consumed in prescribed  
175 fires and wildfires in the United States [*Christian et al.*, 2003; *McMeeking et al.*, 2009] and are listed in  
176 Table 2. They included several species common to maritime chaparral, Sierra Nevada montane, and  
177 southeastern (SE) US coastal plain ecosystems where prescribed fire measurements took place during the  
178 aircraft studies. Fuels burned during laboratory experiments were conditioned in a low humidity chamber  
179 for at least one night prior to being burned, as described by *McMeeking et al.* [2009]; fuel moisture  
180 contents prior to combustion are provided in Table 2. The total fuel mass and the mass of fuel remaining  
181 after combustion were measured as a function of time from ignition using a Mettler-Toledo PM34  
182 balance. Fuels were ignited using a heated wire bed treated with ethanol, as described in *McMeeking et al.*  
183 [2009].

184 We performed the airborne measurements on a US Forest Service DHC-6 Twin Otter aircraft  
185 modified for atmospheric sampling. SLOBB consisted of eight research flights that examined emissions  
186 from six different prescribed fires whose locations in central California are shown in Figure 1a and listed  
187 in Table 1. SCREAM featured nine research flights that examined emissions from prescribed fires at six  
188 locations in South Carolina, shown in Figure 1b and also listed in Table 1. *Akagi et al.* [2012, 2013] and  
189 *Burling et al.* [2011] described the aircraft platform, measurement systems, and fire characteristics during  
190 SLOBB and SCREAM in more detail. The aircraft had a maximum flight endurance of approximately  
191 four hours. Sampling for aerosol measurements was performed through a roof-mounted diffuser inlet  
192 [*Yokelson et al.*, 2007] that was super-isokinetic for typical aircraft sampling speeds (40-80 m s<sup>-1</sup>), with  
193 maximum theoretical losses of 10% for sub-micron particles and < 5% for 0.5 μm diameter particles and  
194 smaller. Super-micron particles were removed via an impactor with a cut-size of 1 μm, so losses or  
195 enhancements of super-micron particles due to the sampling configuration could be neglected.

196 During SLOBB, the aircraft sampled four prescribed fires in maritime chaparral vegetation  
197 (designated as Grant A, Grant B, Williams, and Atmore, based on their location) and two prescribed fires  
198 in Sierra Nevada mixed conifer vegetation (Turtle and Shaver). A detailed description of each fire  
199 including date, fuels, area burned, and trace gas emissions are provided by *Burling et al.* [2011] and in  
200 Table 1 (excluding emissions data), which includes corrected values of burned area for the Grant A and  
201 Grant B fires originally reported by *Burling et al.* [2011]. *Akagi et al.* [2012] described measurements  
202 performed for the Williams Fire, which was the target of two research flights to characterize initial  
203 emissions and subsequent aging processes. The SCREAM aircraft measurements included high-intensity  
204 prescribed fires at the Fort Jackson (FJ) military facility near Columbia, SC. We sampled three fires  
205 located on the facility, referred to as FJ 6, FJ 9b and FJ 22b after the name of the plot of land on the base  
206 where the fire occurred. These burns included detailed inventories of fuels consumed in the fires and  
207 complementary ground-based measurements [*Aurell and Gullett*, 2013; *Yokelson et al.*, 2013a; *Akagi et*  
208 *al.*, 2014]. The second half of the project examined three prescribed fires in the surrounding region  
209 (referred to as Georgetown, Francis Marion and Bamberg based on their location), but since these fires

210 supplemented the FJ work and were not planned in advance, there was less information regarding the  
211 fuels consumed in these fires and no ground-based measurements. Consistent with the airborne smoke  
212 marker measurements of *Sullivan et al.* [2014], our independent data suggest there are two distinct fires at  
213 the Bamberg location; Bamberg A appears likely to be attributed to needles while Bamberg B appears  
214 likely to be attributed to marsh grasses. *Akagi et al.* [2013] described the evolution of trace gases  
215 downwind of the fires investigated during SCREAM; here, we focus on characterization of aerosol  
216 species near the source. Atmospheric evolution of PM during SCREAM will be described in upcoming  
217 work.

## 218 **2.2 Refractory black carbon measurements**

219 The SP2 (DMT, Inc., Boulder, Colorado) measures rBC particle mass using a laser-induced  
220 incandescence technique [*Stephens et al.*, 2003] and has been deployed in a number of aircraft-, ground-  
221 and laboratory-based studies to examine rBC concentrations and properties [e.g., *Baumgardner et al.*,  
222 2004; *Schwarz et al.*, 2006; *Moteki et al.*, 2007; *Liu et al.*, 2011]. The instrument illuminates particles  
223 with an intra-cavity Nd:YAG diode pumped laser ( $\lambda = 1064$  nm) with a Gaussian beam profile. Sampled  
224 particles containing sufficient absorbing material are heated to their vaporization temperature and emit  
225 radiation. While some metals present in biomass burning plumes (e.g., potassium) are strong absorbers at  
226 1064 nm, they are typically in the form of salts (e.g., KCl, K<sub>2</sub>SO<sub>4</sub>), which are non-absorbing [*Yamasoe et*  
227 *al.*, 2000]; furthermore, the absorption must be strong enough to heat the particle to temperatures in the  
228 range 3500-5000 K to be classified as rBC by the SP2 [*Schwarz et al.*, 2006]. The emitted light is  
229 proportional to the rBC mass of individual particles and the exact relationship is determined via  
230 calibration with a known mass of an atmospheric rBC proxy material [*Baumgardner et al.*, 2012]. Several  
231 recent studies have investigated the SP2 response to different rBC proxy materials and found an  
232 approximately 30% variability in response depending on material [e.g., *Moteki and Kondo*, 2010];  
233 furthermore, major atmospheric rBC particle types including diesel emissions, wood smoke, and ambient  
234 aerosol fell within a few percent of the range of responses to proxy materials [e.g., *Laborde et al.*, 2012].

235 In all three campaigns, monodisperse proxy materials were generated via a Collision-type atomizer (TSI  
236 3076; TSI, Inc., Shoreview, MN) and differential mobility analyzer (TSI 3081). We used glassy carbon  
237 spheres (density =  $1.42 \text{ g cm}^{-3}$ ; Alfa Aesar, Ward Hill, MA) as the calibration material during the SLOBB  
238 and FLAME-III campaigns and fullerene soot (density =  $0.5\text{-}0.9 \text{ g cm}^{-3}$ ) during the SCREAM campaign.  
239 The SP2 response to these two materials may differ by up to 20%; however, as there is considerable  
240 variability in recommended calibrations in the limited available literature [e.g., Figure 9 in *Moteki and*  
241 *Kondo*, 2010], we have not applied a correction to our data. A BC density of  $1.8 \text{ g cm}^{-3}$  was assumed  
242 based on *Bond and Bergstrom* [2006] and was used to convert the mass of a single particle to its volume  
243 (assuming spherical particles), similar to *Gysel et al.* [2011].

244 We did not optimize the gain settings on the SP2 incandescence detectors to examine the rBC  
245 vaporization temperature or color ratio over the full size range, but instead improved the sizing resolution  
246 of the system. A faulty amplifier board on the higher gain detector caused a truncation of the  
247 incandescence signal for rBC particles with masses above 6 fg (approximately  $0.18 \mu\text{m}$  mass equivalent  
248 diameter) during the FLAME-III measurements, so only the low-gain detector was used for sizing rBC  
249 particles above this size. Both detectors were fully operational during the aircraft campaigns.

250 During the laboratory campaign, the SP2 sampled emissions alternately downstream of a thermal  
251 denuder or an unperturbed bypass line over 1 minute intervals, [*G.R. McMeeking et al.*, Impacts of non-  
252 refractory light absorption by aerosols from biomass burning, submitted manuscript, 2014], but we  
253 restricted our analysis herein to bypass sampling periods. On the aircraft, the SP2 inlet system was  
254 modified to reduce coincidence errors due to the expected high particle concentrations by providing a  
255 controlled, filtered, and dried dilution airflow of approximately 10:1. The SP2 data analysis procedures  
256 were also modified to account for the high concentrations of particles encountered in smoke plumes.  
257 Modifications included adding a routine to identify when more than one black carbon particle was  
258 detected within the acquisition window and controlling the instrument thresholds for particle detection in  
259 high concentration environments either manually in real-time or in post-processing. Refractory black  
260 carbon mass distributions were fit with lognormal functions to approximate rBC mass outside the

261 instrument detection range (0.070-0.600  $\mu\text{m}$  for rBC “cores” over our assumed density and operating  
262 parameters) and to infer the mass-median diameter of uncoated rBC particles ( $\text{MMD}_{\text{rBC}}$ ). We report all  
263 rBC mass concentrations after adjustments using these lognormal corrections, which typically resulted in  
264 an increase in mass concentration by a factor of 1-1.4. Following *Schwarz et al.* [2006], we assume 10%  
265 uncertainty due to flow calibrations and 20% uncertainty in mass calibration factor; propagated, the net  
266 measurement uncertainty for the SP2 was  $\sim 25\%$ .

### 267 **2.3 Non-refractory sub-micron aerosol measurements**

268 Non-refractory aerosol composition was measured by two Time-of-Flight Aerosol Mass Spectrometers  
269 (ToF-AMS). A compact-ToF-AMS (c-ToF-AMS) [*Drewnick et al.*, 2005] from the California Institute of  
270 Technology flew on the Twin Otter during the SLOBB measurements and a high-resolution-ToF-AMS  
271 (HR-ToF-AMS) [*DeCarlo et al.*, 2006] from Colorado State University was used for the FLAME-III and  
272 SCREAM measurements. The c-ToF-AMS instrument has been deployed on several aircraft-  
273 measurement campaigns and has been described in detail elsewhere [*Murphy et al.*, 2009; *Sorooshian et*  
274 *al.*, 2010]; during SLOBB, the c-ToF-AMS measured composition using ion time-of-flight (iTOF) “V-  
275 mode” in the mass spectrometer for 4 seconds out of every 12 second cycle (the remainder being in  
276 particle time-of-flight, pTOF, mode, data not shown here). During FLAME-III, the HR-ToF-AMS was  
277 operating in alternating iTOF “V-mode” and “W-mode” over 30 second intervals; here, we report only  
278 “V-mode” data. For SCREAM, the HR-ToF-AMS was modified for flight operation by mounting it in  
279 two NSF/NCAR GV-type aircraft racks. The HR-ToF-AMS operated over a 6 second cycle under iTOF  
280 “V-mode”. Data from both instruments were processed using the ToF-AMS software SQUIRREL [*Allan*  
281 *et al.*, 2004; *DeCarlo et al.*, 2006] and PIKA [*Sueper et al.*, 2013] to obtain aerosol mass concentrations  
282 at standard temperature and pressure ( $\mu\text{g sm}^{-3}$ , 273.15 K and 1013.25 hPa). A particle filter (Pall, HEPA  
283 capsule P/N 12144) was placed in front of the AMS at various times throughout the flights to determine  
284 the signal interference from particle-free air. Measurement uncertainty for the mass concentration of each  
285 species was taken to be  $\pm 30\%$  for both AMS datasets [*Bahreini et al.*, 2009].

286 Values of AMS collection efficiency (CE) applied to BB smoke vary in the literature between 0.5  
287 and 1.0 [Weimer *et al.*, 2008; Heringa *et al.*, 2011; Akagi *et al.*, 2012], either based on assumptions made  
288 in prior work or inferred from complementary measurements, which introduces some uncertainty in  
289 reported values. For the FLAME-III laboratory data, we assume a CE = 1, consistent with the treatment of  
290 other biomass burning primary OA data from this study [Hennigan *et al.*, 2011; May *et al.*, 2013; Ortega  
291 *et al.*, 2013]. A constant CE of 0.5 was applied to the c-ToF AMS data based on the traditional approach  
292 for accounting for CE in ambient datasets [Canagaratna *et al.*, 2007] and following the treatment of  
293 SLOBB data in Akagi *et al.* [2012], but the HR-ToF AMS data during SCREAM were processed using a  
294 recently-developed composition-dependent CE (CDCE) algorithm [Middlebrook *et al.*, 2012]. During  
295 SCREAM, the calculated CDCE ranged from 0.5 to nearly 1.0; however, the campaign-average value was  
296 0.53 with higher values for more organic-rich aerosol. Hence, the treatment of both airborne datasets was  
297 roughly equivalent. These assumptions introduce a bias (up to a factor of two) to inter-comparisons  
298 between the laboratory and airborne measurements; however, in both cases, the CE has been either  
299 assumed or estimated, so there is some inherent uncertainty (up to a factor of 2) associated with these  
300 values.

301 For the c-ToF-AMS data analysis, adjustments were made to the default fragmentation table [Allan *et*  
302 *al.*, 2004] for sulfate and nitrate ion fragment signals in the mass spectrum. Under high aerosol loadings,  
303 such as in a smoke plume, the contributions of organic ions with the same nominal mass as inorganic ions  
304 can be higher than in the default fragmentation table. The sulfate ion fragment  $\text{SO}^+$  at  $m/z$  48 has little  
305 interference from organic fragments (even at high aerosol loadings), so the contributions to sulfate from  
306 the three major remaining fragments ( $\text{SO}_2^+$ ,  $\text{SO}_3^+$  and  $\text{H}_2\text{SO}_4^+$ ) were reconstructed based on a linear  
307 relationship with the  $\text{SO}^+$  during a period of low organic interference from the same flight. The nitrate  
308 ion  $\text{NO}^+$  at  $m/z$  30 also has organic interference, and was reconstructed in a similar manner with the other  
309 main nitrate ion,  $\text{NO}_2^+$  at  $m/z$  46 [Bae *et al.*, 2007]. For the HR-ToF-AMS, these issues do not apply, since  
310 it can usually resolve the inorganic and organic ions at the same nominal mass. Hereafter, we will simply  
311 refer to both the c-ToF-AMS and HR-ToF-AMS measurements as AMS measurements.

## 312 2.4 Trace gas measurements

313 During the laboratory campaign, mixing ratios of CO and CO<sub>2</sub> were measured by a variable-range  
314 gas filter correlation analyzer (Thermo Environmental Model 48C; Thermo Fisher Scientific, Inc.,  
315 Waltham, MA) and a non-dispersive infrared (NDIR) gas analyzer (Li-Cor Model 6262; Li-Cor  
316 Biosciences, Lincoln, NE), respectively. The gas analyzers were calibrated with standards of known  
317 concentrations before and after each burn experiment. The estimated accuracy/precision of the  
318 measurements were 1%/0.1% for CO<sub>2</sub> and 2%/1% for CO [McMeeking *et al.*, 2009]. During SLOBB  
319 aircraft measurements, CO<sub>2</sub> mixing ratios were measured continuously by the NDIR gas analyzer at 0.5-1  
320 Hz from the same inlet as the SP2. During the SCREAM aircraft measurements, CO<sub>2</sub>, CO, CH<sub>4</sub> and water  
321 vapor mixing ratios were measured by a cavity ring-down spectrometer (CRDS; Picarro G2401; Picarro,  
322 Inc., Santa Clara, CA), calibrated in-flight with mixed CO/CO<sub>2</sub>/CH<sub>4</sub> standards, following Urbanski  
323 [2013].

324 An airborne Fourier transform infrared spectrometer system (AFTIR) collected “grab” samples  
325 outside and inside of the smoke plumes [Burling *et al.*, 2011; Akagi *et al.*, 2013]. Sample spectra were  
326 analyzed to determine mixing ratios of CO, CO<sub>2</sub>, and additional gas-phase compounds described  
327 elsewhere [Burling *et al.*, 2011; Akagi *et al.*, 2012, 2013]. The AFTIR system detection limits ranged  
328 from 1-10 ppbv for most species depending on the spectral averaging time.

## 329 2.5 Sampling and analysis procedures

330 The aircraft sampling procedure varied from flight-to-flight, but the following general approach  
331 was used to characterize the fire emissions in most situations. The aircraft first sampled “fresh” emissions  
332 at the fire source over a range of altitudes up to a few thousand meters for up to two hours, and if air  
333 traffic control restrictions permitted, flew downwind of the fire to sample the aged but still relatively  
334 young emissions in a quasi-Lagrangian manner. Examples of flight tracks are provide elsewhere [Akagi *et al.*  
335 *al.*, 2012, 2013]. Concentrations of the various species were measured across each plume intercept to  
336 obtain plume-integrated values. The measurements near the source were used to determine the emission

337 ratios and emission factors for each species, as described below. There was no discernable effect of  
338 altitude on emission ratios or emission factors.

339 During the laboratory campaign, the excess mixing ratios (denoted by  $\Delta$ ) were calculated by  
340 subtracting the background concentrations of CO, CO<sub>2</sub>, rBC and AMS-measured components in the time  
341 interval immediately prior to fuel ignition. The background CO<sub>2</sub> concentrations drifted slightly during  
342 each experiment, so there was some subjectivity and resulting uncertainty in calculating  $\Delta$ CO<sub>2</sub>,  
343 particularly for fires that did not emit much CO<sub>2</sub>. During aircraft measurements, time-dependent  
344 background concentrations were collected outside of the plume, as the background values varied with  
345 location over the duration of the flight.

346 Excess CO and CO<sub>2</sub> molar mixing ratios were used to determine the modified combustion  
347 efficiency (MCE) [Yokelson *et al.*, 1996]:

$$348 \quad MCE = \frac{\Delta CO_2}{\Delta CO_2 + \Delta CO} \quad (1)$$

349 Higher MCE values indicate a greater contribution from flaming combustion emissions and lower MCE  
350 values indicate a greater contribution from smoldering combustion emissions. We estimated the  
351 uncertainty in MCE during FLAME-III arising from the uncertainty in the background CO<sub>2</sub> mixing ratio  
352 by comparing two independent calculations of MCE by separate project investigators (this work and  
353 *Hennigan et al.* [2011]). Agreement between the two measurements diverged as  $\Delta$ CO<sub>2</sub> decreased due to  
354 low  $\Delta$ CO<sub>2</sub> signal-to-noise over the background CO<sub>2</sub> value. Differences in calculated MCE between the  
355 two independent approaches ranged from roughly 0.5% for MCE of 0.94-0.97 to roughly 2% for MCE of  
356 0.87-0.90.

357 Fire-averaged mass ER for each species (X) were either directly calculated from the mass ratio of  
358  $\Delta$ X to  $\Delta$ CO for emissions sampled in the laboratory or from the regression of the plume-integrated source  
359 samples during the aircraft measurements, with the y-intercept forced through zero, since all data were  
360 background-corrected. Emission factors (EF), which relate the mass of X emitted to the mass of dry fuel  
361 consumed, were calculated using the carbon mass balance method [Ward and Hardy, 1991]. In this work,

362 we report both ER and EF; both can be used to estimate total fresh emissions, and they are  
363 interchangeable if the emission factor of CO ( $EF_{CO}$ ) is known. As plumes dilute, their concentrations  
364 normalized to CO can be compared to ER as a probe of physicochemical evolution [*de Gouw et al.*, 2008;  
365 *Bahreini et al.*, 2009; *DeCarlo et al.*, 2010; *Akagi et al.*, 2013]. Furthermore, CO is a more robust tracer  
366 for long-range transport of biomass burning emissions [e.g., *Yokelson et al.*, 2009; *Cubison et al.*, 2011]  
367 since  $CO_2$  may be lost due to uptake by plants and bodies of water. The use of ER also removes the need  
368 for any *a priori* knowledge of the sampled fire that are required to calculate EF (e.g., carbon content of  
369 the fuel) or implement EF into chemical transport models (e.g., area burned, fuel loading within the area,  
370 fraction of fuel consumed).

371         Measurements of  $\Delta CO$  and  $\Delta CO_2$  were used to estimate the total carbon emitted during the  
372 laboratory experiments, but the aircraft total carbon estimates also included carbon in gases measured by  
373 the AFTIR system. Neglecting carbon mass in compounds not detected by the AFTIR system and in  
374 particles generally over-estimates the emission factors by only 1-2% due to the small amount of carbon  
375 present in particles and gases other than  $CH_4$ , CO and  $CO_2$ , although in certain cases, carbon contained in  
376 the aerosol and non-methane organic gases can represent a non-negligible contribution [*Watson et al.*,  
377 2011; *Yokelson et al.*, 2013a]. For the airborne measurements described during this work, CO and  $CO_2$   
378 represented >97% of total measured carbon emissions [*Burling et al.*, 2011; *Akagi et al.*, 2013]. Fuel  
379 carbon mass fraction ( $F_C$ ), on a dry mass of fuel basis, was measured for laboratory fuels (Table 2) based  
380 on the combustion method [*Allen et al.*, 1974] and was assumed to be 50% for unknown fuels burned  
381 during the subset of prescribed fires that did not have fuel measurements. The measured carbon content in  
382 fuels similar to those consumed in the fires sampled during the SLOBB and SCREAM airborne studies  
383 ranged from 48-55% [*McMeeking et al.*, 2009; *Burling et al.*, 2011].

### 384 3. Results and discussion

385 We grouped the prescribed fires and fuels burned in the laboratory by ecosystem type as listed in  
386 Table 2. The prescribed fires measured during SLOBB took place in maritime chaparral and Sierra  
387 Nevada montane ecosystems and the prescribed fires measured during SCREAM all occurred in the  
388 southeastern US coastal plain ecosystem. The fuels tested during FLAME-III included several species  
389 from these ecosystems, namely manzanita, chamise, and ceanothus (chaparral), ponderosa and lodgepole  
390 pine (montane) and gallberry, turkey oak, wiregrass and the pocosin composite sample (SE coastal plain).  
391 We also burned several fuels during FLAME-III from ecosystems not sampled with the aircraft. Note that  
392 for all FLAME-III experiments, we examined fire-integrated or fire-averaged emissions, rather than real-  
393 time emission data.

394 The fire-integrated MCE values observed over the duration of the burn during the FLAME-III  
395 laboratory measurements ranged between approximately 0.85-0.96, reflecting the variability in  
396 combustion conditions from burn to burn. MCE values measured at various plume locations during the  
397 aircraft campaigns ranged between 0.89-0.95 during SLOBB and 0.92-0.97 during SCREAM. This  
398 variability between laboratory and aircraft measurements may be due to natural variability in MCE caused  
399 by fuel composition, moisture content, or loading; or due to laboratory measurements representing fire-  
400 integrated values (i.e., over all combustion phases). Further, *Akagi et al.* [2014] compared ground- and  
401 airborne-measurements of MCE during SCREAM and found that ground-level MCE was roughly 10%  
402 less than the airborne MCE; hence, the emissions aloft may be more influenced by flaming combustion.  
403 Nevertheless, we relied on the MCE to attempt to account for differences in combustion conditions when  
404 comparing aircraft and laboratory measurements of particle emissions in the following sections. MCE  
405 cannot, however, explain all of the variance in emissions, so there was residual variance due to the other  
406 factors listed above (e.g., fuel composition, fuel loading).

407 In the subsequent sections, we report emission ratios of  $\Delta r_{BC}$  to  $\Delta CO$  ( $ER_{r_{BC}}$ ) with units of ng  
408  $r_{BC} \text{ sm}^{-3} \text{ ppbv-CO}^{-1}$ , following the standard convention in SP2 literature. However, we report emission

409 ratios of other aerosol constituents on a mass basis (e.g.,  $ER_{OA} = [g\ OA\ g\text{-}CO^{-1}]$ ). To convert reported  
410  $ER_{rBC}$  to mass ratios, the reader should apply a factor of  $8.7 \times 10^{-4}$  to convert our reported values of  $ng\ sm^{-3}$   
411  $ppbv\text{-}CO^{-1}$  to  $g\ rBC\ g\text{-}CO^{-1}$ . All emission factors are reported as  $g\ kg\text{-}dry\text{-}fuel\text{-}consumed^{-1}$  (hereafter,  
412 shortened to  $g\ kg\text{-}fuel^{-1}$  but still indicating  $kg\text{-}dry\text{-}fuel\text{-}consumed$ ). For each ecosystem/campaign, we  
413 report values as average  $\pm$  one standard deviation ( $1\sigma$ ), unless otherwise noted. Further, we refer to two-  
414 tailed  $p$ -values from unpaired  $t$ -tests providing comparisons between laboratory and airborne data simply  
415 as “ $p$ -values” for brevity; however, in all cases, the number of samples used in the  $t$ -test calculations are  
416 small ( $\leq 6$ ), so additional data are required to increase the strength of these statistical comparisons.

### 417 **3.1 Refractory black carbon emissions**

#### 418 **3.1.1 rBC emission ratios**

419 Since the absolute concentrations of an emitted species measured over a fire depend on dilution  
420 and fuel consumption rates, we used emission ratios to aid the comparison of emissions from different  
421 fires. Values of  $ER_{rBC}$  for 27 laboratory burns and prescribed fires are listed in Table 3 and also shown in  
422 Figure 2 plotted against MCE. They ranged from approximately 0 to  $40\ ng\ rBC\ sm^{-3}\ ppbv\text{-}CO^{-1}$  and  
423 tended to be lowest for laboratory burns characterized by predominantly smoldering combustion and  
424 highest for laboratory burns dominated by flaming combustion. The chaparral fires had the highest  
425 average  $ER_{rBC}$  values, with laboratory values of  $24.7 \pm 2.4\ ng\ rBC\ sm^{-3}\ ppbv\text{-}CO^{-1}$  and aircraft values of  
426  $21.9 \pm 5.8\ ng\ rBC\ sm^{-3}\ ppbv\text{-}CO^{-1}$ . We have excluded the Atmore fire from this, and subsequent, averages  
427 for chaparral fires as it was a very small ( $\sim 10$  ha) coastal fire, and it was considered to be an statistical  
428 outlier, having an rBC-to-OA ratio that was roughly 23 standard deviations greater than the average for  
429 the other aircraft data (Grant A, Grant B, Williams). The montane fuels had the lowest  $ER_{rBC}$ , emitting  $2.8$   
430  $\pm 1.9\ ng\ rBC\ sm^{-3}\ ppbv\text{-}CO^{-1}$  in the laboratory and  $6.5 \pm 0.3\ ng\ rBC\ sm^{-3}\ ppbv\text{-}CO^{-1}$  during airborne  
431 sampling. Southeastern US coastal plain fuels and fires had a laboratory-measured  $ER_{rBC}$  of  $15.8 \pm 5.7\ ng$   
432  $BC\ sm^{-3}\ ppbv\text{-}CO^{-1}$  and an aircraft-measured  $ER_{rBC}$  of  $17.9 \pm 9.5\ ng\ rBC\ sm^{-3}\ ppbv\text{-}CO^{-1}$ . The relatively  
433 good agreement observed between laboratory- and aircraft-measured emissions of rBC from chaparral

434 and SE coastal plain fires ( $p$ -values = 0.453 and 0.630, respectively) provides some confidence in the  
435 representativeness of using the laboratory emission measurements to predict rBC emissions in the absence  
436 of field data. We note also that, within a fuel class, the MCE varied between laboratory and field data; for  
437 example, the average laboratory MCE for chaparral fuels was roughly 0.025 greater than the average  
438 MCE measured above chaparral prescribed fires. Since rBC emissions depend on MCE, we expect some  
439 variability due to this factor.

440 The aircraft-measured  $ER_{rBC}$  for montane prescribed fires were roughly a factor of two higher  
441 than the laboratory measurements (Table 3), which is the largest discrepancy among all laboratory/field  
442 comparisons for rBC ( $p$ -value = 0.046), although we are only comparing six laboratory-derived values to  
443 two airborne-derived values. Possible causes of this difference include, but may not be limited to, the  
444 following: 1) laboratory MCE for montane fuels was slightly lower than MCE measured in the aircraft for  
445 this ecosystem (0.891 versus 0.899); 2) only pine needles and branches were burned in the laboratory for  
446 montane ecosystem fuels, while shrub-layer species and downed dead wood were burned during the two  
447 prescribed fires; 3) the structure of the fuel bed in the laboratory is better maintained for shrubs and  
448 grasses compared to trees; and 4) emissions of OA were sometimes very high in the laboratory (see  
449 discussion in Section 3.3 below), and the unidentified factors driving high OA may have also resulted in  
450 low rBC. For example, both *Chen et al.* [2010] and *Hayashi et al.* [2014] observe some decreases in EC  
451 emissions for fuels with increased moisture content.. Hence, it is likely that the laboratory burns were not  
452 fully representative of the prescribed fires for these four reasons, although differences in fuels consumed  
453 and fuel moisture content (related to the fourth item in the list) may be most important. Conversely,  
454 chaparral and southeastern prescribed fires tended to burn grasses and shrubs that were also studied in the  
455 laboratory; average field and laboratory  $ER_{rBC}$  for these fires agreed within 13% (excluding Atmore) for  
456 chaparral and 12% for southeastern prescribed fires (relative percent difference).

457 Refractory black carbon is emitted by flaming combustion, so we expected higher emissions from  
458 fires that had a larger MCE, as indicated in Figure 2. The relationship between  $ER_{rBC}$  and MCE was  
459 generally consistent for both laboratory- and aircraft-measured fires, suggesting laboratory and prescribed

460 fires produced similar amounts of rBC relative to CO for similar MCE, despite all the differences between  
461 the conditions in the laboratory and the field. Hence, MCE appears to be a useful parameter for describing  
462 the variability in  $ER_{rBC}$  measured for different fires, so inter-comparisons of  $ER_{rBC}$  from different studies  
463 should be accompanied by MCE as a diagnostic.

### 464 3.1.2 rBC emission factors

465 Emission factors for rBC ( $EF_{rBC}$ ) for the laboratory and prescribed fire emissions are listed in  
466 Table 4 and shown as a function of MCE in Figure 3a. Laboratory fires had the largest range in  $EF_{rBC}$ ,  
467 with some producing little measurable rBC above background concentrations and others emitting as much  
468 as 2.7 g rBC kg-fuel<sup>-1</sup>. Ecosystem-averaged  $EF_{rBC}$  measured from the aircraft were  $1.43 \pm 0.13$  g kg-fuel<sup>-1</sup>  
469 for chaparral (excluding Atmore),  $0.59 \pm 0.13$  g kg-fuel<sup>-1</sup> for montane, and  $1.11 \pm 0.67$  g kg-fuel<sup>-1</sup> for SE  
470 coastal plain prescribed fires. Emission factors had a similar relationship with MCE as was observed for  
471  $ER_{rBC}$ , again reflecting the role of flaming combustion in the production of rBC; however, the coefficient  
472 of determination ( $R^2$ ) value of a global linear regression of these data was only 0.265, suggesting that  
473 other factors likely affect the variability in the emission factors.

### 474 3.1.3 Comparison to prior measurements

475 There are few studies that have used the SP2 to measure rBC emissions from fires or from  
476 prescribed fires specifically. *Kondo et al.* [2011b] measured rBC with an SP2 in a number of smoke  
477 plumes over North America, as summarized in Figure 2. They report average  $ER_{rBC}$  values of  $11.8 \pm 4.5$   
478 ng rBC sm<sup>-3</sup> ppbv-CO<sup>-1</sup> in plumes originating from Asia (MCE =  $0.985 \pm 0.002$ ),  $3.25 \pm 0.678$  ng rBC sm<sup>-3</sup>  
479 ppbv-CO<sup>-1</sup> for plumes originating from Canada (MCE =  $0.846 \pm 0.060$ ), and  $2.86 \pm 0.35$  ng rBC sm<sup>-3</sup>  
480 ppbv-CO<sup>-1</sup> for plumes originating in California (MCE =  $0.961 \pm 0.021$ ). MCE calculated from excess CO<sub>2</sub>  
481 and CO for highly aged and dilute plumes (e.g., Asian plumes sampled over North America), are more  
482 uncertain compared to measurements near the source where CO and CO<sub>2</sub> are highly elevated above  
483 background levels [*Yokelson et al.*, 2013b]. If the calculated MCE was too large due to uncertainties with  
484 long-range transport (e.g., as  $\Delta CO_2$  and  $\Delta CO$  approach zero, and hence, excess-signal-to-noise decreases),

485 this may potentially explain the discrepancy between the *Kondo et al.* [2011b]  $ER_{rBC}$  measurements and  
486 our observations. The only other aircraft-based rBC measurements of which we are aware were made by  
487 *Schwarz et al.* [2008], who intercepted two smoke plumes over Texas they attributed to brush fires, *Sahu*  
488 *et al.* [2012], who sampled fire plumes over California, and *Dahlkötter et al.* [2014], who detected  
489 biomass burning plumes transported from North America over Europe. *Schwarz et al.* [2008] observed an  
490  $ER_{rBC}$  of  $22.3 \pm 1.5 \text{ ng BC sm}^{-3} \text{ ppbv-CO}^{-1}$  averaged over three plume intercepts, similar to our  
491 observations over California chaparral fires, while *Sahu et al.* [2012] observed much lower  $ER_{rBC}$  of  $3.28$   
492  $\pm 0.97 \text{ ng rBC sm}^{-3} \text{ ppbv-CO}^{-1}$ . The data from these previous studies have also been included in Figure 2  
493 and compare reasonably well to our data when the effects of MCE are considered; *Dahlkötter et al.*  
494 [2014] do not report  $ER_{rBC}$  in their work. As a point of reference, urban/fossil fuel  $ER_{rBC}$  reported in the  
495 literature range from roughly 1.5-7  $\text{ng rBC sm}^{-3} \text{ ppbv-CO}^{-1}$  [*Baumgardner et al.*, 2007; *Schwarz et al.*,  
496 2008; *McMeeking et al.*, 2010; *Subramanian et al.*, 2010; *Sahu et al.*, 2012].

497 Emission ratios measured for aged emissions may also be influenced by the removal of BC from  
498 the smoke plume due to wet and dry deposition processes. Both our study and the *Schwarz et al.* [2008]  
499 measurements were restricted to emissions sampled within an hour of emission. The *Kondo et al.* [2011b]  
500 observations included much older smoke plumes, but they also restricted their analysis to samples that  
501 had minimal influence from precipitation based on an analysis of backward trajectories. *Sahu et al.* [2012]  
502 do not report sample age, but they sampled biomass burning emissions from wildfires in California during  
503 a flight campaign over California, restricting their data to those with excess acetonitrile (a gas-phase  
504 tracer for biomass burning) greater than 300 pptv. Possible reasons for differences between the aged  
505 plumes in previous work and our measurements of young plumes include the previously discussed higher  
506 uncertainty in determining MCE from small  $\Delta CO_2$  values relative to background  $CO_2$  in more aged  
507 plumes and differences in fuels or fire size (small prescribed fires versus large wildfires). The first  
508 possibility is supported by the fact that the  $ER_{rBC}$  reported by both studies overlapped, but MCE did not.

509 Most previous measurements used to derive emission factors or emission ratios for BC from fire  
510 relied on filter-based optical or thermal-optical methods to quantify BC and have been summarized in

511 several reviews [*Andreae and Merlet*, 2001; *Bond et al.*, 2004, 2013; *Akagi et al.*, 2011]. The classic  
512 review of *Andreae and Merlet* [2001] recommended a literature-averaged  $EF_{BC}$  of  $0.56 \pm 0.19$  g kg-fuel<sup>-1</sup>  
513 for extra-tropical forests, which is commonly used in emission inventories and chemical transport models  
514 [*van der Werf et al.*, 2010; *Akagi et al.*, 2011]. Many of our laboratory- and aircraft-measured emission  
515 factors for rBC from biomass burning were greater than one standard deviation above the recommended  
516 average from *Andreae and Merlet* [2001], especially for chaparral and SE coastal plain fuels (see Table  
517 4); however, this value from *Andreae and Merlet* [2001] includes emissions from boreal fires, which we  
518 expect to be similar to our montane fires. Comparing  $EF_{rBC}$  to emission factors of EC ( $EF_{EC}$ ) from  
519 *McMeeking et al.* [2009], who studied similar ecosystems/fuels as the present work,  $EF_{rBC}$  from the  
520 present study are generally greater than  $EF_{EC}$  by roughly a factor of 1.5-3.0, as shown in Figure 3a.  
521 Similarly, for on-road motor vehicles, *Liggio et al.* [2012] propose that BC is under-estimated in existing  
522 emission inventories for mobile sources, based on comparisons of their SP2 measurements and previous  
523 filter-based measurements. We speculate that, in general, this discrepancy may be related to an over-  
524 correction for OC pyrolysis in OC/EC analysis methods rather than errors in the photo-absorption  
525 methods for determining BC; however, we lack systematic comparisons between methods for biomass  
526 burning samples during our study. We emphasize that BC and EC are both operationally-defined and are  
527 not necessarily equivalent. The only systematic inter-comparisons of differences between EC/BC  
528 measurement techniques of which we are aware are: *Watson et al.* [2005], who review prior EC/BC  
529 studies that demonstrate differences in mass concentrations up to a factor of 7; *Kondo et al.* [2011a],  
530 who demonstrate good agreement between different methods, although this finding is sensitive to their  
531 inferred BC mass absorption cross-section; and *Yelverton et al.* [2014], who demonstrate that measured  
532 EC/BC mass concentrations measured via different instruments may vary up to a factor of 2. Our results,  
533 in conjunction with previous work and regardless of the reason (e.g., systematic differences between  
534 instruments/analyses, larger available dataset with greater natural variability), suggest that  $EF_{BC}$  may  
535 require further upward revision in emission inventories, although additional measurements, particularly  
536 for wildfires, are needed to confirm this hypothesis. This statement is consistent with the upper

537 uncertainty bound for BC proposed by *Bond et al.* [2013], who estimate that  $EF_{BC}$  currently used in  
538 emission inventories may be biased low by up to a factor of four.

### 539 **3.2 Refractory black carbon mass median diameters**

540 Sizing information is critical to accurately predict aerosol microphysical and optical properties in  
541 models. Here, we report the  $MMD_{rBC}$  (described in Section 2.2) for both laboratory and aircraft  
542 measurements. We calculated fire-averaged  $MMD_{rBC}$  for all plumes intercepted within 5 km of the fire  
543 location to restrict our analysis of aircraft data to relatively fresh emissions. During the FLAME-III  
544 laboratory burns, we used the average  $MMD_{rBC}$  observed during the same time period used to determine  
545 emission ratios and emission factors near the beginning of each experiment.

546 Laboratory-measured  $MMD_{rBC}$  ranged from between 0.14-0.19  $\mu\text{m}$ , with the exception of that  
547 measured for emissions from Alaskan duff, which had an  $MMD_{rBC}$  of 0.12  $\mu\text{m}$ . The Alaskan duff burn  
548 emitted very little rBC and was the only laboratory burn where it was difficult to distinguish between the  
549 background rBC and the rBC emitted by the fire, so we excluded this fuel from the following analyses.  
550 The average  $MMD_{rBC}$  of all fuels, excluding the duff, was  $0.17 \pm 0.02 \mu\text{m}$ . There was no clear  
551 relationship between  $MMD_{rBC}$  and fuel type, MCE, or total rBC mass emitted. Refractory BC MMD  
552 shifted to larger particle sizes in emissions from the coastal plain prescribed fires measured over South  
553 Carolina during SCREAM, with a campaign average  $\pm 1\sigma$  of  $0.22 \pm 0.01 \mu\text{m}$ . These aircraft-measured  
554  $MMD_{rBC}$  were roughly 30% larger than those measured in the laboratory (average laboratory SE coastal  
555 plain fuel  $MMD_{rBC} = 0.17 \pm 0.01 \mu\text{m}$ ), but were consistent with previous SP2 measurements of biomass  
556 burning rBC. For example, *Schwarz et al.* [2008] observed a  $MMD_{rBC}$  of 0.21  $\mu\text{m}$  for the biomass burning  
557 plume encountered over Texas. *Kondo et al.* [2011b] observed  $MMD_{rBC}$  values of 0.21  $\mu\text{m}$  and 0.19  $\mu\text{m}$   
558 for biomass burning emissions from Asia and Canada, respectively, while *Sahu et al.* [2012] reported  
559 average  $MMD_{rBC}$  of  $0.20 \pm 0.02 \mu\text{m}$ . Both *Kondo et al.* [2011b] and *Sahu et al.* [2012] values have been  
560 adjusted using our assumed rBC density of  $1.8 \text{ g cm}^{-3}$ . Conversely, *Dahlkötter et al.* [2014] reported a  
561 range of  $MMD_{rBC}$  from 0.12-0.15  $\mu\text{m}$  for a smoke plume that had undergone long-range transport from

562 North America to Europe; these  $MMD_{rBC}$  are more similar to our laboratory studies, but the exact cause  
563 of the difference between these measurements and other plume measurements is unknown. Nevertheless,  
564 the comparison of our results with prior work highlights the variability in  $MMD_{rBC}$ , which can bound  
565 aerosol microphysical and optical processes in predictive model simulations.

### 566 **3.3 Non-refractory aerosol emissions**

#### 567 **3.3.1 Emission ratios**

568 The emission ratios for the major AMS-measured non-refractory sub-micron aerosol components  
569 are listed in Table 3. Figure 4 shows an example of the regressions used to determine the emission ratios  
570 for non-refractory aerosol (as well as rBC) during the Fort Jackson plot 22b prescribed fire (2 November  
571 2011). Each point represents a single plume interception that was measured during the flight and that was  
572 confirmed as a plume hit via a spike in CRDS CO within 5 km of the fire location. An ordinary least-  
573 squares regression, forcing the intercept through zero, was used to derive the slope best representing the  
574 data, with this slope used to infer the ER [Yokelson *et al.*, 1999]; we expect the intercept to be zero since  
575 all values are background-corrected locally. In the laboratory, background OA concentrations were  
576 generally  $< 5 \mu\text{g m}^{-3}$ , while in the field, background OA concentrations range from roughly 5-15  $\mu\text{g m}^{-3}$ .  
577 Observed emission ratios for organic aerosol ( $ER_{OA}$ ) were generally higher during montane prescribed  
578 fires than during SE coastal plain fires and chaparral fires, with average values of  $0.10 \pm 0.01 \text{ g OA g-CO}^{-1}$   
579 <sup>1</sup>. We observed lower average values of  $0.037 \pm 0.016 \text{ g OA g-CO}^{-1}$  over SE coastal fires and  $0.048 \pm$   
580  $0.026 \text{ g OA g-CO}^{-1}$  over chaparral fires (excluding Atmore). Cubison *et al.* [2011] summarized recent  
581 measurements of  $ER_{OA}$  and concluded that  $ER_{OA}$  can range from approximately 0.04-0.15  $\text{g OA g-CO}^{-1}$   
582 for non-aged emissions, while Jolleys *et al.* [2012] report a larger range of  $ER_{OA}$  of 0.02-0.33  $\text{g OA g-CO}^{-1}$   
583 <sup>1</sup> for various aircraft campaigns, both being consistent with the range of values we observed over our  
584 prescribed fires.

585 Laboratory-measured  $ER_{OA}$  represented a much larger range of values compared to the aircraft  
586 measurements, ranging from  $0.021 \pm 0.018 \text{ g OA g-CO}^{-1}$  for chaparral species to  $0.15 \pm 0.13 \text{ g OA g-CO}^{-1}$

587 for SE coastal plain species to  $1.14 \pm 0.30$  g OA g-CO<sup>-1</sup> for montane species. Laboratory and airborne  
588 ER<sub>OA</sub> from chaparral fires differ by roughly a factor of two; this could potentially be related to the  
589 assumed AMS CE for the field data. However, an unpaired *t*-test (excluding the Atmore fire as described  
590 above) suggests this difference is not statistically significant (two-tailed *p* value = 0.164).

591         The values for montane fuels are well over ten times our aircraft observations and reported  
592 literature values for extratropical/pine understory forests [Akagi *et al.*, 2011; Yokelson *et al.*, 2013a],  
593 which is a statistically-significant difference (*p*-value = 0.0036). We attribute the factor of 5-10 difference  
594 between airborne and laboratory-derived ER<sub>OA</sub> for montane and SE coastal plain fuels (*p*-value = 0.054)  
595 to a) high fuel moisture content and b) gas-to-particle partitioning of semi-volatile material at high OA  
596 mass concentrations, similar to May *et al.* [2013]; assumed values of AMS CE may also play a role, but  
597 neither can wholly explain these differences. During FLAME-III, initial fuel moisture contents relative to  
598 dry fuel mass prior to fuel conditioning ranged from roughly 45-75% for lodgepole and ponderosa pines;  
599 both Chen *et al.* [2010] and Hayashi *et al.* [2014] observed that OC emissions and fuel moisture content  
600 were positively correlated, suggesting that laboratory-derived emission factors may be biased high partly  
601 due to pre-ignition pyrolysis emissions of OA in the presence of high fuel moisture. We expect the  
602 moisture content of the fine dead fuels during the Turtle and Shaver burns to be roughly 10%, as targeted  
603 in the Turtle burn plan, which is roughly a factor of 7 lower than in the laboratory; furthermore, nearby  
604 meteorological stations indicated that neither site received any precipitation in the 17 days preceding the  
605 prescribed fire. Similarly, laboratory SE coastal plain fuels with moisture contents of roughly 10% were  
606 generally consistent with our airborne observations, while those laboratory fuels with greater fuel  
607 moisture contents were generally larger than our airborne observations. Hence, high residual water in the  
608 fuel prior to combustion may explain the very large ER<sub>OA</sub> for montane fuels in our study.

609         However, our observations may also be biased by the fact that primary OA emitted from fires has  
610 been observed to be semi-volatile, and thus, will vary non-linearly with dilution [Lipsky and Robinson,  
611 2006; Grieshop *et al.*, 2009a; Huffman *et al.*, 2009; May *et al.*, 2013]; that is, higher OA concentrations  
612 will draw additional semi-volatile organic vapors into the particle phase in order to maintain

613 thermodynamic equilibrium [Donahue *et al.*, 2006; Robinson *et al.*, 2010]. Laboratory fires that produced  
614 the highest  $ER_{OA}$  also had the highest OA mass concentrations (e.g., montane species). The fire-averaged  
615 mass concentrations in the laboratory chamber for the montane fuels were  $4620 \pm 1430 \mu\text{g sm}^{-3}$  compared  
616 to average plume-integrated OA mass concentrations of  $185 \pm 15 \mu\text{g sm}^{-3}$  observed on the aircraft over  
617 montane prescribed fires. A similar argument likely explains the roughly factor of 4 difference between  
618 SE coastal fuels studied during FLAME-III and the aircraft sampling during SCREAM. Furthermore,  
619  $ER_{OA}$  will also be sensitive to  $ER_{tot}$ , the emission ratio of all semi-volatile organics (representing both the  
620 gas and particle phase) that may undergo gas-particle partitioning [Robinson *et al.*, 2010; May *et al.*,  
621 2013].  $ER_{tot}$  can be estimated using derived volatility distributions, such as that presented as a laboratory  
622 composite by May *et al.* [2013]. However, to our knowledge, this is one of three volatility distributions  
623 derived for biomass burning OA emissions thus far (with the others being Cappa and Jimenez [2010],  
624 which was derived from AMS positive matrix factorization results, and Grieshop *et al.* [2009a], which  
625 was derived from emissions from a wood stove); none of these volatility distributions have been widely  
626 confirmed as representative of biomass burning emissions in the field, so we do not provide estimates of  
627  $ER_{tot}$  in this work. We simply note that  $ER_{OA}$  is expected to be greater when OA concentrations are larger  
628 and to decrease with dilution.

### 629 **3.3.2 Emission factors**

630 As with the rBC emissions, we converted the emission ratios of measured OA to emission factors  
631 using  $EF_{CO}$  and provide them in Table 4 and Figure 3b (note the split axis). As with emission ratios, OA  
632 emission factors ( $EF_{OA}$ ) were generally the highest of all the measured aerosol species. Average aircraft-  
633 measured  $EF_{OA}$  were  $3.9 \pm 1.8 \text{ g OA kg-fuel}^{-1}$  for chaparral fires (excluding the Atmore fire, as discussed  
634 in Section 3.1),  $11.2 \pm 2.7 \text{ g OA kg-fuel}^{-1}$  for montane fires and  $2.8 \pm 1.6 \text{ g OA kg-fuel}^{-1}$  for SE coastal  
635 plain fires. Results for the SE coastal plain differ than those previously reported by Akagi *et al.* [2013]  
636 due to an updated analysis of the AMS data.

637           These results indicate that fresh organic aerosols emissions from fires can be highly variable,  
638 even within the same ecosystem, consistent with previous work [*McMeeking et al.*, 2009; *Akagi et al.*,  
639 2011; *Hosseini et al.*, 2013]. This variability is also observed in the laboratory data for a given ecosystem;  
640 for example, the average  $EF_{OA}$  for SE coastal plain fuels were  $11.5 \pm 13.8$  g OA kg-fuel<sup>-1</sup> during the  
641 laboratory portion of this study.  $EF_{OA}$  were anti-correlated with MCE, as expected for smoldering  
642 combustion and as also demonstrated for laboratory burns by *McMeeking et al.* [2009], although the  
643 strength of this relationship can be degraded by gas-particle partitioning effects. We also compare the  
644  $EF_{OA}$  data to the linear fit for  $EF_{OC}$  from *McMeeking et al.* [2009] in Figure 3b, after converting OC to  
645 OA using OA:OC ratios of 1.2 (reduced hydrocarbons as reported in *Turpin and Lim* [2001]), 1.6 (the  
646 approximate average value from two biomass fuels reported in *Aiken et al.* [2008]), and 2.0 (the  
647 approximate value reported for fireplace wood in *Turpin and Lim* [2001]). This converted linear fit agrees  
648 with some of the FLAME-III data (namely, those with higher fuel moisture contents that were not  
649 montane fuels), but not other FLAME-III data or the airborne data. This variable agreement may be, in  
650 part, due to the only modest  $R^2$  between MCE and  $EF_{OC}$  reported in *McMeeking et al.* [2009] (0.36); for  
651 our data, we calculate an  $R^2$  value of 0.47.. However, fuel moisture content and OA loading also play a  
652 role on the magnitude of  $EF_{OA}$ , which will increase the apparent variability in the MCE versus  $EF_{OA}$   
653 relationship. These dependencies of EF on fuel moisture content and OA mass concentrations suggest that  
654 future laboratory studies should report both fire-averaged OA loading and fuel moisture contents in  
655 addition to ER and/or EF in order to accurately extrapolate laboratory data into chemical transport models  
656 used to simulate air quality impacts of wildfires.

657           Figure 3c-f and Table 4 also provide EF for sub-micron non-refractory inorganic aerosol species  
658 measured by the AMS ( $SO_4^{2-}$ ,  $NO_3^-$ ,  $NH_4^+$ , and  $Chl^-$ ) as a function of MCE. In general, inorganic EF were  
659 weakly dependent on MCE, in contrast to rBC and OA, and appeared to have a greater dependence on the  
660 type of fuel burned; values of  $R^2$  were 0.049, 0.547, 0.047, and 0.025 for  $SO_4^{2-}$ ,  $NO_3^-$ ,  $NH_4^+$ , and  $Chl^-$ ,  
661 respectively, suggesting that among these species, only  $NO_3^-$  exhibits a dependency on MCE. For  
662 example, grasses burned in the laboratory and during prescribed burns (Georgetown fire) tended to have

663 higher  $\text{Chl}^-$  EF, consistent with typically higher fuel chlorine content compared to other fuels [Lobert *et*  
664 *al.*, 1999]. Similarly, both Christian *et al.* [2003] and Hosseini *et al.* [2013] found a strong relationship  
665 between fuel chlorine content and chloride-containing particulate emissions for a series of laboratory  
666 fires. We lack detailed fuel composition information to perform a similar analysis for the aircraft studies,  
667 but such a fuel-composition-dependence is consistent with our results.

668 Our aircraft measurements provide some estimates of inorganic emissions for prescribed fires for  
669 several ecosystems, as summarized in Table 4. While we lack a mechanistic driver of the factors  
670 controlling the emissions variability (e.g., fuel chemistry), presumably the elevated  $\text{NO}_3^-$  EF for some of  
671 the FLAME-III montane fuels are related to elevated fuel nitrogen content, similar to  $\text{Chl}^-$ . Note that we  
672 only include species reliably quantified by the standard AMS operation and analysis, so we may be  
673 excluding some refractory salts (e.g., potassium chloride KCl) that do not vaporize readily in the  
674 instrument. However, the  $\text{Chl}^-$  emission factors reported in Table 4 are in reasonable agreement with  
675 filter-based data from previous studies that investigated fuels from chaparral, montane, and SE coastal  
676 plain ecosystems [McMeeking *et al.*, 2009; Hosseini *et al.*, 2013], so it is unlikely that any  $\text{Chl}^-$  is missing  
677 from our samples, even if we are not detecting the  $\text{K}^+$  that it may have been paired with in the particles.

### 678 **3.4 Total aerosol emissions**

679 We combined our measurements of rBC and non-refractory sub-micron aerosol components to  
680 investigate the variability in aerosol composition emitted from prescribed fires. Figure 5 shows mass  
681 fractions for each species relative to total measured sub-micron PM ( $\text{PM}_1$ ), calculated from the sum of  
682 SP2 rBC and AMS-measured non-refractory species. The FLAME-III results presented in this figure from  
683 combined SP2 and AMS measurements are qualitatively similar to filter-based results for repeated fuels  
684 investigated during previous FLAME studies [Levin *et al.*, 2010]. The laboratory fires produced a wide  
685 range of aerosol compositions, which we loosely classified into high OA, high rBC, high rBC +  $\text{SO}_4^{2-}$  and  
686 high  $\text{Chl}^-$  groups. High OA emitters were mostly pines and dense fuels such as duff and peat, which all  
687 had higher fuel moisture contents. Most other fuels emitted higher mass fractions of rBC (10-60%).

688 Chaparral fuels tended to emit higher mass fractions of  $\text{SO}_4^{2-}$  while grass fuels emitted relatively high  
689 mass fractions of  $\text{Cl}^-$ . Prescribed fire emissions rarely had inorganic mass fractions as high as observed  
690 in the laboratory; the only exceptions were the prescribed grass fire (Georgetown fire) that emitted  
691 relatively high mass fractions of  $\text{Cl}^-$  and  $\text{NH}_4^+$  and the Bamberg fires which had large amounts of  $\text{NO}_3^-$   
692 and  $\text{SO}_4^{2-}$ . The exact cause of these discrepancies between the laboratory and field is largely unknown.

693 Some mass fractions of rBC between laboratory burns and prescribed fires did not agree very  
694 well. For example, the montane pine species studied during FLAME-III have nearly negligible rBC  
695 fractions, while the PM from the Shaver and Turtle fires were roughly 5% rBC; the main driver of this  
696 discrepancy was likely the very high OA emissions that dominated total PM during these laboratory fires.  
697 Some of this difference may be due to differences in OA concentrations and the fuel burned in the field  
698 versus the laboratory. Conversely, chaparral prescribed fires generally had the highest rBC emissions  
699 while laboratory fuels such as ceanothus, chamise, and manzanita, which were combusted during the  
700 chaparral fires [Burling *et al.*, 2011], generally had the highest rBC mass fractions in the emissions  
701 measured during FLAME-III.

702 In Tables 3 and 4, we also provide ER and EF for  $\text{PM}_{10}$ . For our aircraft data, SE US coastal plain  
703 fires had the lowest average  $\text{PM}_{10}$  EF ( $4.4 \pm 2.0 \text{ g kg-fuel}^{-1}$ ) emission factors, followed by chaparral  
704 (excluding Atmore) ( $\text{PM}_{10}$  EF =  $5.5 \pm 1.7 \text{ g kg-fuel}^{-1}$ ) and montane ( $\text{PM}_{10}$  EF =  $12.1 \pm 2.9 \text{ g kg-fuel}^{-1}$ )  
705 fires. Based on  $\text{PM}_{2.5}$  measurements in prior work [McMeeking *et al.*, 2009; Hosseini *et al.*, 2013], these  
706 estimates of  $\text{PM}_{10}$  may be biased low by roughly 1-10% due to missing potassium; furthermore, Levin *et*  
707 *al.* [2010] report that emissions of refractory salts (e.g., KCl,  $\text{K}_2\text{SO}_4$ , NaCl) and minerals (e.g., calcium  
708 oxide) may represent up to 50% of the emitted particle mass, depending on fuel type. The differences  
709 between ecosystems were mainly due to differences in OA emissions, which represented the majority of  
710 the emitted  $\text{PM}_{10}$ . Our aircraft observations of  $\text{PM}_{10}$  were approximately within the range of values of  $12.7$   
711  $\pm 7.5 \text{ g kg-fuel}^{-1}$  recommended by Akagi *et al.* [2011] for  $\text{PM}_{2.5}$  emitted by temperate forests. Our data  
712 also highlight the substantial natural variability in fire emissions due to differences in ecosystems, fuel  
713 moisture content, fire intensity, and vegetation cover; for example, the relative standard deviation

714 (standard deviation divided by the average) for the ecosystems that we considered ranged from 0.24 for  
715 montane fires to 0.45 for SE US coastal plain fires.

## 716 **4. Conclusions**

717 In this paper we report measured EFs and ERs for key sub-micron aerosol components in emissions from  
718 prescribed burns in three US ecosystems (chaparral, montane and SE coastal plain) and compare with EFs  
719 and ERs for similar fuels measured in some open laboratory burns. Refractory black carbon aerosol was  
720 measured using a laser-induced incandescence technique (SP2) rather than the more traditional filter-  
721 based absorption/thermal-optical methods, with measured  $EF_{rBC}$  ranging from approximately 0-3 g  
722  $kg\text{-fuel}^{-1}$  depending on fuel and combustion conditions.  $EF_{rBC}$  measured in the laboratory were consistent  
723 with those measured in the field from the aircraft, suggesting laboratory-derived values can adequately  
724 represent larger-scale fires when MCE is used to characterize the burn conditions. Organic aerosol  
725 emissions measured in the laboratory had a much wider range of observed values ( $EF_{OA} = <1\text{-}200$  g  $kg\text{-}$   
726  $fuel^{-1}$ ) compared to aircraft measurements ( $EF_{OA} = 0.2\text{-}13$  g  $kg\text{-fuel}^{-1}$ ) and appeared to depend strongly on  
727 fuel moisture content and the OA mass concentration, as suggested by *May et al.* [2013], as well as MCE,  
728 although there were some exceptions. The evolution of OA with dilution and atmospheric processing will  
729 affect its concentrations downwind of source regions and remains a topic of active research (e.g., see  
730 *Hennigan et al.* [2011], *May et al.* [2013], *Ortega et al.* [2013], and *E.J.T. Levin et al.* [in preparation] for  
731 analysis of FLAME-III data; *A.A. May et al.* [in preparation] for analysis of SCREAM data; and *Akagi et*  
732 *al.* [2012] for analysis of SLOBB data). Inorganic emission factors were always smaller than rBC and OA  
733 emission factors and depended somewhat on fuel type, though fuels burned in the laboratory tended to  
734 emit relatively higher mass fractions of inorganics compared to prescribed fires measured in the field.  
735 One notable exception was relatively high chloride mass fraction in emissions measured over a prescribed  
736 coastal grass fire in South Carolina.

737 It is of interest to compare the range of observed  $ER_{rBC}$  for our biomass burning samples with  
738 those reported for other BC sources, which are primarily contained combustion such as vehicular and  
739 industrial emissions [Bond *et al.*, 2013]. Spackman *et al.* [2008] compared the biomass burning plume  
740 measurements described in Schwarz *et al.* [2008] to regional urban and industrial plumes observed over  
741 Texas and found lower  $ER_{rBC}$  ( $7.5 \text{ ng BC sm}^{-3} \text{ ppbv-CO}^{-1}$ ) for the urban emissions compared to biomass  
742 burning emissions. Others have also reported similar and/or lower  $ER_{rBC}$  for urban regions [Baumgardner  
743 *et al.*, 2007; McMeeking *et al.*, 2010; Subramanian *et al.*, 2010; Sahu *et al.*, 2012]. Although the  
744 ecosystem-averaged  $ER_{rBC}$  values we observed for chaparral and SE coastal plain fires and the Schwarz *et al.*  
745 *et al.* [2008] observations were 2-3 times higher than the largest observed urban  $ER_{rBC}$  ratios, our montane  
746 fire values and the  $ER_{rBC}$  values reported by Kondo *et al.* [2011b] fall within the range of reported urban  
747  $ER_{rBC}$ . Thus  $ER_{rBC}$  alone is not a sufficient parameter for distinguishing between biomass burning and  
748 urban BC sources in modeling studies, and their relative contributions to an ambient sample cannot be  
749 determined without additional information (e.g., MCE) on the characteristics of the prescribed or wild fire  
750 considered.

751 The SP2-derived EF and ER for refractory black carbon in this work are consistently higher than  
752 previously reported values based on filter sampling with absorption/thermal-optical analyses, which may  
753 suggest that EF and ER for rBC in existing emissions inventories may require an increase via the  
754 inclusion of these newer, SP2-derived data in the average inventory values. However, systematic  
755 intercomparisons between the SP2 and filter-based techniques are required to confirm the robustness of  
756 this finding to determine whether this is a systematic difference or natural variability. Additional studies,  
757 especially in important biomass burning regions in the tropics, are needed to determine whether this  
758 revision is needed for all ecosystems or only for those studied in this work.

## 759 **Acknowledgements**

760 We thank the USFS Twin Otter pilots Bill Mank and Scott Miller and mechanic Steve Woods for their  
761 contribution to the SLOBB and SCREAM campaigns and the USFS JeffCo aircraft base, San Luis

762 Aviation, Eagle Aviation, the NSF/NCAR Research Aviation Facility and Ezra Levin for their  
763 contributions to the installation of instruments on the Twin Otter and its deployment to the field.  
764 Adaptation of the Twin Otter for atmospheric measurements and other support was provided by NSF  
765 grants ATM-0531055 and ATM-0936321 to R.Y. Prescribed fires were organized and carried out by John  
766 Maitland and forestry staff at Fort Jackson and Dan Ardoin at Vandenberg AFB. We also thank Jason  
767 McCarty of the Santa Barbara County Fire Department for conducting burns and providing fuels and  
768 weather information during SLOBB. Fuel inventories and other ground-based information were provided  
769 by Jim Reardon, Aaron Sparks and Signe Leirfallom. We thank the USFS Fire Science Laboratory staff  
770 and the FLAME-III participants for their contributions to the laboratory measurements. We also thank  
771 Shane Murphy, Roya Bahreini, and Ann Middlebrook for their suggestions and assistance in modifying  
772 the Colorado State University AMS for aircraft operation during SCREAM; furthermore, Tim Onasch,  
773 Jose Jimenez, and Misha Schurman all contributed to discussions regarding AMS analysis of the  
774 SCREAM data. G. R. McMeeking's participation in FLAME-III was supported by the UK Royal Society.  
775 The California aircraft measurements were supported by the Strategic Environmental Research and  
776 Development Program (SERDP) projects SI-1648 and SI-1649 and the SP2 was supported by the UK  
777 Natural Environment Research Council (NERC). We acknowledge funding from the Joint Fire Science  
778 Program under project JFSP 11-1-5-12 for the South Carolina aircraft measurements and related AMS  
779 data analysis. The Fort Jackson study was supported by SERDP project RC-1649 administered partly  
780 through the Forest Service Research Joint Venture Agreement 08JV11272166039. Additional flight hours  
781 and SCREAM CRDS data were provided by Joint Fire Science Program project 08-1-6-09. To request  
782 copies of the data used in this paper, please contact the corresponding author. Finally, we would like to  
783 thank our editor, Lynn Russell, as well as the anonymous reviewers for their useful comments.

## 784 5. References

- 785 Aiken, A. C. et al. (2008), O/C and OM/OC Ratios of Primary, Secondary, and Ambient Organic  
786 Aerosols with High-Resolution Time-of-Flight Aerosol Mass Spectrometry, *Environ. Sci. Technol.*,  
787 42(12), 4478–4485, doi:10.1021/es703009q.
- 788 Akagi, S. K., R. J. Yokelson, C. Wiedinmyer, M. J. Alvarado, J. S. Reid, T. Karl, J. D. Crouse, and P. O.  
789 Wennberg (2011), Emission factors for open and domestic biomass burning for use in atmospheric  
790 models, *Atmos. Chem. Phys.*, 11(9), 4039–4072, doi:10.5194/acp-11-4039-2011.
- 791 Akagi, S. K. et al. (2012), Evolution of trace gases and particles emitted by a chaparral fire in California,  
792 *Atmos. Chem. Phys.*, 12(3), 1397–1421, doi:10.5194/acp-12-1397-2012.
- 793 Akagi, S. K. et al. (2013), Measurements of reactive trace gases and variable O<sub>3</sub> formation rates in some  
794 South Carolina biomass burning plumes, *Atmos. Chem. Phys.*, 13(3), 1141–1165, doi:10.5194/acp-  
795 13-1141-2013.
- 796 Akagi, S. K., I. R. Burling, A. Mendoza, T. J. Johnson, M. Cameron, D. W. T. Griffith, C. Paton-Walsh,  
797 D. R. Weise, J. Reardon, and R. J. Yokelson (2014), Field measurements of trace gases emitted by  
798 prescribed fires in southeastern US pine forests using an open-path FTIR system, *Atmos. Chem.*  
799 *Phys.*, 14(1), 199–215, doi:10.5194/acp-14-199-2014.
- 800 Allan, J. D. et al. (2004), A generalised method for the extraction of chemically resolved mass spectra  
801 from Aerodyne aerosol mass spectrometer data, *J. Aerosol Sci.*, 35(7), 909–922,  
802 doi:10.1016/j.jaerosci.2004.02.007.
- 803 Allen, S. E., H. M. Grimshaw, J. A. Parkinson, and C. Quarmbury (1974), *Chemical analysis of ecological*  
804 *materials*, Blackwell Scientific, Oxford, UK.
- 805 Andreae, M. O., and A. Gelencsér (2006), Black carbon or brown carbon? The nature of light-absorbing  
806 carbonaceous aerosols, *Atmos. Chem. Phys.*, 6(10), 3131–3148, doi:10.5194/acp-6-3131-2006.
- 807 Andreae, M. O., and P. Merlet (2001), Emission of trace gases and aerosols from biomass burning,  
808 *Global Biogeochem. Cycles*, 15(4), 955–966, doi:10.1029/2000GB001382.
- 809 Aurell, J., and B. K. Gullett (2013), Emission factors from aerial and ground measurements of field and  
810 laboratory forest burns in the southeastern US: PM<sub>2.5</sub>, black and brown carbon, VOC, and  
811 PCDD/PCDF., *Environ. Sci. Technol.*, 47(15), 8443–52, doi:10.1021/es402101k.
- 812 Bae, M.-S., J. J. Schwab, Q. Zhang, O. Hogrefe, K. L. Demerjian, S. Weimer, K. Rhoads, D. Orsini, P.  
813 Venkatchari, and P. K. Hopke (2007), Interference of organic signals in highly time resolved  
814 nitrate measurements by low mass resolution aerosol mass spectrometry, *J. Geophys. Res.*,  
815 112(D22), D22305, doi:10.1029/2007JD008614.
- 816 Bahreini, R. et al. (2009), Organic aerosol formation in urban and industrial plumes near Houston and  
817 Dallas, Texas, *J. Geophys. Res.*, 114, D00F16, doi:10.1029/2008JD011493.

- 818 Baumgardner, D., G. L. Kok, and G. B. Raga (2004), Warming of the Arctic lower stratosphere by light  
819 absorbing particles, *Geophys. Res. Lett.*, *31*(6), L06117, doi:10.1029/2003GL018883.
- 820 Baumgardner, D., G. L. Kok, and G. B. Raga (2007), On the diurnal variability of particle properties  
821 related to light absorbing carbon in Mexico City, *Atmos. Chem. Phys.*, *7*(10), 2517–2526,  
822 doi:10.5194/acp-7-2517-2007.
- 823 Baumgardner, D. et al. (2012), Soot reference materials for instrument calibration and intercomparisons: a  
824 workshop summary with recommendations, *Atmos. Meas. Tech.*, *5*(8), 1869–1887, doi:10.5194/amt-  
825 5-1869-2012.
- 826 Bond, T. C., and R. W. Bergstrom (2006), Light Absorption by Carbonaceous Particles: An Investigative  
827 Review, *Aerosol Sci. Technol.*, *40*(1), 27–67, doi:10.1080/02786820500421521.
- 828 Bond, T. C., D. G. Streets, K. F. Yarber, S. M. Nelson, J. H. Woo, and Z. Klimont (2004), A technology-  
829 based global inventory of black and organic carbon emissions from combustion, *J. Geophys. Res.*,  
830 *109*(D14), D14203, doi:10.1029/2003JD003697.
- 831 Bond, T. C. et al. (2013), Bounding the role of black carbon in the climate system: A scientific  
832 assessment, *J. Geophys. Res. Atmos.*, *118*(11), 5380–5552, doi:10.1002/jgrd.50171.
- 833 Burling, I. R., R. J. Yokelson, S. K. Akagi, S. P. Urbanski, C. E. Wold, D. W. T. Griffith, T. J. Johnson, J.  
834 Reardon, and D. R. Weise (2011), Airborne and ground-based measurements of the trace gases and  
835 particles emitted by prescribed fires in the United States, *Atmos. Chem. Phys.*, *11*(23), 12197–  
836 12216, doi:10.5194/acp-11-12197-2011.
- 837 Canagaratna, M. R. et al. (2007), Chemical and microphysical characterization of ambient aerosols with  
838 the aerodyne aerosol mass spectrometer., *Mass Spectrom. Rev.*, *26*(2), 185–222,  
839 doi:10.1002/mas.20115.
- 840 Capes, G., B. Johnson, G. McFiggans, P. I. Williams, J. Haywood, and H. Coe (2008), Aging of biomass  
841 burning aerosols over West Africa: Aircraft measurements of chemical composition, microphysical  
842 properties, and emission ratios, *J. Geophys. Res.*, *113*, D00C15, doi:10.1029/2008JD009845.
- 843 Cappa, C. D., and J. L. Jimenez (2010), Quantitative estimates of the volatility of ambient organic  
844 aerosol, *Atmos. Chem. Phys.*, *10*(12), 5409–5424, doi:10.5194/acp-10-5409-2010.
- 845 Cappa, C. D., D. A. Lack, J. B. Burkholder, and A. R. Ravishankara (2008), Bias in Filter-Based Aerosol  
846 Light Absorption Measurements Due to Organic Aerosol Loading: Evidence from Laboratory  
847 Measurements, *Aerosol Sci. Technol.*, *42*(12), 1022–1032, doi:10.1080/02786820802389285.
- 848 Carter, M. C., and C. D. Foster (2004), Prescribed burning and productivity in southern pine forests: a  
849 review, *For. Ecol. Manage.*, *191*(1-3), 93–109, doi:10.1016/j.foreco.2003.11.006.
- 850 Chen, L.-W. A., P. Verburg, A. Shackelford, D. Zhu, R. Susfalk, J. C. Chow, and J. G. Watson (2010),  
851 Moisture effects on carbon and nitrogen emission from burning of wildland biomass, *Atmos. Chem.*  
852 *Phys.*, *10*(14), 6617–6625, doi:10.5194/acp-10-6617-2010.

- 853 Chow, J. C., J. G. Watson, L.-W. A. Chen, W. P. Arnott, H. Moosmüller, and K. Fung (2004),  
854 Equivalence of Elemental Carbon by Thermal/Optical Reflectance and Transmittance with Different  
855 Temperature Protocols, *Environ. Sci. Technol.*, 38(16), 4414–4422, doi:10.1021/es034936u.
- 856 Chow, J. C., J. G. Watson, L.-W. A. Chen, M. C. O. Chang, N. F. Robinson, D. Trimble, and S. Kohl  
857 (2007), The IMPROVE\_A Temperature Protocol for Thermal/Optical Carbon Analysis: Maintaining  
858 Consistency with a Long-Term Database, *J. Air Waste Manage. Assoc.*, 57(9), 1014–1023,  
859 doi:10.3155/1047-3289.57.9.1014.
- 860 Christian, T. J., B. Kleiss, R. J. Yokelson, R. Holzinger, P. J. Crutzen, W. M. Hao, B. H. Saharjo, and D.  
861 E. Ward (2003), Comprehensive laboratory measurements of biomass-burning emissions: 1.  
862 Emissions from Indonesian, African, and other fuels, *J. Geophys. Res.*, 108(D23), 4719,  
863 doi:10.1029/2003JD003704.
- 864 Cubison, M. J. et al. (2011), Effects of aging on organic aerosol from open biomass burning smoke in  
865 aircraft and laboratory studies, *Atmos. Chem. Phys.*, 11(23), 12049–12064, doi:10.5194/acp-11-  
866 12049-2011.
- 867 Dahlkötter, F., M. Gysel, D. Sauer, A. Minikin, R. Baumann, P. Seifert, A. Ansmann, M. Fromm, C.  
868 Voigt, and B. Weinzierl (2014), The Pagami Creek smoke plume after long-range transport to the  
869 upper troposphere over Europe – aerosol properties and black carbon mixing state, *Atmos. Chem.*  
870 *Phys.*, 14(12), 6111–6137, doi:10.5194/acp-14-6111-2014.
- 871 DeCarlo, P. F. et al. (2006), Field-deployable, high-resolution, time-of-flight aerosol mass spectrometer.,  
872 *Anal. Chem.*, 78(24), 8281–9, doi:10.1021/ac061249n.
- 873 DeCarlo, P. F. et al. (2008), Fast airborne aerosol size and chemistry measurements above Mexico City  
874 and Central Mexico during the MILAGRO campaign, *Atmos. Chem. Phys.*, 8(14), 4027–4048,  
875 doi:10.5194/acp-8-4027-2008.
- 876 DeCarlo, P. F. et al. (2010), Investigation of the sources and processing of organic aerosol over the  
877 Central Mexican Plateau from aircraft measurements during MILAGRO, *Atmos. Chem. Phys.*,  
878 10(12), 5257–5280, doi:10.5194/acp-10-5257-2010.
- 879 Donahue, N. M., A. L. Robinson, C. O. Stanier, and S. N. Pandis (2006), Coupled Partitioning, Dilution,  
880 and Chemical Aging of Semivolatile Organics, *Environ. Sci. Technol.*, 40(8), 2635–2643,  
881 doi:10.1021/es052297c.
- 882 Drewnick, F. et al. (2005), A New Time-of-Flight Aerosol Mass Spectrometer (TOF-AMS)—Instrument  
883 Description and First Field Deployment, *Aerosol Sci. Technol.*, 39(7), 637–658,  
884 doi:10.1080/02786820500182040.
- 885 Engelhart, G. J., C. J. Hennigan, M. A. Miracolo, A. L. Robinson, and S. N. Pandis (2012), Cloud  
886 condensation nuclei activity of fresh primary and aged biomass burning aerosol, *Atmos. Chem.*  
887 *Phys.*, 12(15), 7285–7293, doi:10.5194/acp-12-7285-2012.
- 888 Fernandes, P. M., and H. S. Botelho (2003), A review of prescribed burning effectiveness in fire hazard  
889 reduction, *Int. J. Wildl. Fire*, 12(2), 117, doi:10.1071/WF02042.

- 890 Flannigan, M. D., M. A. Krawchuk, W. J. de Groot, B. M. Wotton, and L. M. Gowman (2009),  
891 Implications of changing climate for global wildland fire, *Int. J. Wildl. Fire*, 18(5), 483,  
892 doi:10.1071/WF08187.
- 893 Formenti, P., W. Elbert, W. Maenhaut, J. Haywood, S. Osborne, and M. O. Andreae (2003), Inorganic  
894 and carbonaceous aerosols during the Southern African Regional Science Initiative (SAFARI 2000)  
895 experiment: Chemical characteristics, physical properties, and emission data for smoke from African  
896 biomass burning, *J. Geophys. Res.*, 108(D13), 8488, doi:10.1029/2002JD002408.
- 897 Giglio, L., J. T. Randerson, and G. R. van der Werf (2013), Analysis of daily, monthly, and annual burned  
898 area using the fourth-generation global fire emissions database (GFED4), *J. Geophys. Res.*  
899 *Biogeosciences*, 118(1), 317–328, doi:10.1002/jgrg.20042.
- 900 De Gouw, J. A. et al. (2008), Sources of particulate matter in the northeastern United States in summer: 1.  
901 Direct emissions and secondary formation of organic matter in urban plumes, *J. Geophys. Res.*,  
902 113(D8), D08301, doi:10.1029/2007JD009243.
- 903 Grieshop, A. P., M. A. Miracolo, N. M. Donahue, and A. L. Robinson (2009a), Constraining the  
904 Volatility Distribution and Gas-Particle Partitioning of Combustion Aerosols Using Isothermal  
905 Dilution and Thermodynamic Measurements, *Environ. Sci. Technol.*, 43(13), 4750–4756,  
906 doi:10.1021/es8032378.
- 907 Grieshop, A. P., J. M. Logue, N. M. Donahue, and A. L. Robinson (2009b), Laboratory investigation of  
908 photochemical oxidation of organic aerosol from wood fires 1: measurement and simulation of  
909 organic aerosol evolution, *Atmos. Chem. Phys.*, 9(4), 1263–1277, doi:10.5194/acp-9-1263-2009.
- 910 Gysel, M., M. Laborde, J. S. Olfert, R. Subramanian, and A. J. Gröhn (2011), Effective density of  
911 Aquadag and fullerene soot black carbon reference materials used for SP2 calibration, *Atmos. Meas.*  
912 *Tech.*, 4(12), 2851–2858, doi:10.5194/amt-4-2851-2011.
- 913 Hayashi, K., K. Ono, M. Kajiura, S. Sudo, S. Yonemura, A. Fushimi, K. Saitoh, Y. Fujitani, and K.  
914 Tanabe (2014), Trace gas and particle emissions from open burning of three cereal crop residues:  
915 Increase in residue moistness enhances emissions of carbon monoxide, methane, and particulate  
916 organic carbon, *Atmos. Environ.*, doi:10.1016/j.atmosenv.2014.06.023.
- 917 Hecobian, A. et al. (2011), Comparison of chemical characteristics of 495 biomass burning plumes  
918 intercepted by the NASA DC-8 aircraft during the ARCTAS/CARB-2008 field campaign, *Atmos.*  
919 *Chem. Phys.*, 11(24), 13325–13337, doi:10.5194/acp-11-13325-2011.
- 920 Heilman, W. E., Y. Liu, S. Urbanski, V. Kovalev, and R. Mickler (2014), Wildland fire emissions,  
921 carbon, and climate: Plume rise, atmospheric transport, and chemistry processes, *For. Ecol.*  
922 *Manage.*, 317, 70–79, doi:10.1016/j.foreco.2013.02.001.
- 923 Hennigan, C. J. et al. (2011), Chemical and physical transformations of organic aerosol from the photo-  
924 oxidation of open biomass burning emissions in an environmental chamber, *Atmos. Chem. Phys.*,  
925 11(15), 7669–7686, doi:10.5194/acp-11-7669-2011.
- 926 Hennigan, C. J., D. M. Westervelt, I. Riipinen, G. J. Engelhart, T. Lee, J. L. Collett, S. N. Pandis, P. J.  
927 Adams, and A. L. Robinson (2012), New particle formation and growth in biomass burning plumes:

928 An important source of cloud condensation nuclei, *Geophys. Res. Lett.*, 39(9), L09805,  
929 doi:10.1029/2012GL050930.

930 Heringa, M. F., P. F. DeCarlo, R. Chirico, T. Tritscher, J. Dommen, E. Weingartner, R. Richter, G.  
931 Wehrle, A. S. H. Prévôt, and U. Baltensperger (2011), Investigations of primary and secondary  
932 particulate matter of different wood combustion appliances with a high-resolution time-of-flight  
933 aerosol mass spectrometer, *Atmos. Chem. Phys.*, 11(12), 5945–5957, doi:10.5194/acp-11-5945-  
934 2011.

935 Hosseini, S. et al. (2013), Laboratory characterization of PM emissions from combustion of wildland  
936 biomass fuels, *J. Geophys. Res. Atmos.*, 118(17), 9914–9929, doi:10.1002/jgrd.50481.

937 Hu, Y., M. T. Odman, M. E. Chang, W. Jackson, S. Lee, E. S. Edgerton, K. Baumann, and A. G. Russell  
938 (2008), Simulation of Air Quality Impacts from Prescribed Fires on an Urban Area, *Environ. Sci.  
939 Technol.*, 42(10), 3676–3682, doi:10.1021/es071703k.

940 Huffman, J. A., K. S. Docherty, C. Mohr, M. J. Cubison, I. M. Ulbrich, P. J. Ziemann, T. B. Onasch, and  
941 J. L. Jimenez (2009), Chemically-Resolved Volatility Measurements of Organic Aerosol from  
942 Different Sources, *Environ. Sci. Technol.*, 43(14), 5351–5357, doi:10.1021/es803539d.

943 Jimenez, J. L. et al. (2009), Evolution of organic aerosols in the atmosphere., *Science*, 326(5959), 1525–9,  
944 doi:10.1126/science.1180353.

945 Jolleys, M. D. et al. (2012), Characterizing the aging of biomass burning organic aerosol by use of mixing  
946 ratios: a meta-analysis of four regions., *Environ. Sci. Technol.*, 46(24), 13093–102,  
947 doi:10.1021/es302386v.

948 Kirchstetter, T. W., T. Novakov, and P. V. Hobbs (2004), Evidence that the spectral dependence of light  
949 absorption by aerosols is affected by organic carbon, *J. Geophys. Res.*, 109(D21), D21208,  
950 doi:10.1029/2004JD004999.

951 Koch, D. et al. (2009), Evaluation of black carbon estimations in global aerosol models, *Atmos. Chem.  
952 Phys.*, 9(22), 9001–9026, doi:10.5194/acp-9-9001-2009.

953 Kondo, Y., L. Sahu, N. Moteki, F. Khan, N. Takegawa, X. Liu, M. Koike, and T. Miyakawa (2011a),  
954 Consistency and Traceability of Black Carbon Measurements Made by Laser-Induced  
955 Incandescence, Thermal-Optical Transmittance, and Filter-Based Photo-Absorption Techniques,  
956 *Aerosol Sci. Technol.*, 45(2), 295–312, doi:10.1080/02786826.2010.533215.

957 Kondo, Y. et al. (2011b), Emissions of black carbon, organic, and inorganic aerosols from biomass  
958 burning in North America and Asia in 2008, *J. Geophys. Res.*, 116(D8), D08204,  
959 doi:10.1029/2010JD015152.

960 Laborde, M., P. Mertes, P. Zieger, J. Dommen, U. Baltensperger, and M. Gysel (2012), Sensitivity of the  
961 Single Particle Soot Photometer to different black carbon types, *Atmos. Meas. Tech.*, 5(5), 1031–  
962 1043, doi:10.5194/amt-5-1031-2012.

- 963 Lack, D. A., and C. D. Cappa (2010), Impact of brown and clear carbon on light absorption enhancement,  
964 single scatter albedo and absorption wavelength dependence of black carbon, *Atmos. Chem. Phys.*,  
965 *10*(9), 4207–4220, doi:10.5194/acp-10-4207-2010.
- 966 Lack, D. A., C. D. Cappa, D. S. Covert, T. Baynard, P. Massoli, B. Sierau, T. S. Bates, P. K. Quinn, E. R.  
967 Lovejoy, and A. R. Ravishankara (2008), Bias in Filter-Based Aerosol Light Absorption  
968 Measurements Due to Organic Aerosol Loading: Evidence from Ambient Measurements, *Aerosol*  
969 *Sci. Technol.*, *42*(12), 1033–1041, doi:10.1080/02786820802389277.
- 970 Lack, D. A., J. M. Langridge, R. Bahreini, C. D. Cappa, A. M. Middlebrook, and J. P. Schwarz (2012),  
971 Brown carbon and internal mixing in biomass burning particles., *Proc. Natl. Acad. Sci. U. S. A.*,  
972 *109*(37), 14802–7, doi:10.1073/pnas.1206575109.
- 973 Levin, E. J. T. et al. (2010), Biomass burning smoke aerosol properties measured during Fire Laboratory  
974 at Missoula Experiments (FLAME), *J. Geophys. Res.*, *115*(D18), D18210,  
975 doi:10.1029/2009JD013601.
- 976 Lewis, K., W. P. Arnott, H. Moosmüller, and C. E. Wold (2008), Strong spectral variation of biomass  
977 smoke light absorption and single scattering albedo observed with a novel dual-wavelength  
978 photoacoustic instrument, *J. Geophys. Res.*, *113*(D16), D16203, doi:10.1029/2007JD009699.
- 979 Liggio, J., M. Gordon, G. Smallwood, S.-M. Li, C. Stroud, R. Staebler, G. Lu, P. Lee, B. Taylor, and J. R.  
980 Brook (2012), Are emissions of black carbon from gasoline vehicles underestimated? Insights from  
981 near and on-road measurements., *Environ. Sci. Technol.*, *46*(9), 4819–28, doi:10.1021/es2033845.
- 982 Lipsky, E. M., and A. L. Robinson (2006), Effects of Dilution on Fine Particle Mass and Partitioning of  
983 Semivolatile Organics in Diesel Exhaust and Wood Smoke, *Environ. Sci. Technol.*, *40*(1), 155–162,  
984 doi:10.1021/es050319p.
- 985 Liu, D. et al. (2011), Carbonaceous aerosols contributed by traffic and solid fuel burning at a polluted  
986 rural site in Northwestern England, *Atmos. Chem. Phys.*, *11*(4), 1603–1619, doi:10.5194/acp-11-  
987 1603-2011.
- 988 Liu, Y., S. Goodrick, G. Achtemeier, W. A. Jackson, J. J. Qu, and W. Wang (2009), Smoke incursions  
989 into urban areas: simulation of a Georgia prescribed burn, *Int. J. Wildl. Fire*, *18*(3), 336,  
990 doi:10.1071/WF08082.
- 991 Lobert, J. M., W. C. Keene, J. A. Logan, and R. Yevich (1999), Global chlorine emissions from biomass  
992 burning: Reactive Chlorine Emissions Inventory, *J. Geophys. Res.*, *104*(D7), 8373,  
993 doi:10.1029/1998JD100077.
- 994 Magi, B. I. (2009), Chemical apportionment of southern African aerosol mass and optical depth, *Atmos.*  
995 *Chem. Phys.*, *9*(19), 7643–7655, doi:10.5194/acp-9-7643-2009.
- 996 May, A. A., E. J. T. Levin, C. J. Hennigan, I. Riipinen, T. Lee, J. L. Collett, J. L. Jimenez, S. M.  
997 Kreidenweis, and A. L. Robinson (2013), Gas-particle partitioning of primary organic aerosol  
998 emissions: 3. Biomass burning, *J. Geophys. Res. Atmos.*, *118*(19), 11,327–11,338,  
999 doi:10.1002/jgrd.50828.

- 1000 McMeeking, G. R. et al. (2006), Smoke-impacted regional haze in California during the summer of 2002,  
1001 *Agric. For. Meteorol.*, 137(1-2), 25–42, doi:10.1016/j.agrformet.2006.01.011.
- 1002 McMeeking, G. R. et al. (2009), Emissions of trace gases and aerosols during the open combustion of  
1003 biomass in the laboratory, *J. Geophys. Res.*, 114(D19), D19210, doi:10.1029/2009JD011836.
- 1004 McMeeking, G. R. et al. (2010), Black carbon measurements in the boundary layer over western and  
1005 northern Europe, *Atmos. Chem. Phys.*, 10(19), 9393–9414, doi:10.5194/acp-10-9393-2010.
- 1006 Middlebrook, A. M., R. Bahreini, J. L. Jimenez, and M. R. Canagaratna (2012), Evaluation of  
1007 Composition-Dependent Collection Efficiencies for the Aerodyne Aerosol Mass Spectrometer using  
1008 Field Data, *Aerosol Sci. Technol.*, 46(3), 258–271, doi:10.1080/02786826.2011.620041.
- 1009 Miller, J. D., H. D. Safford, M. Crimmins, and A. E. Thode (2008), Quantitative Evidence for Increasing  
1010 Forest Fire Severity in the Sierra Nevada and Southern Cascade Mountains, California and Nevada,  
1011 USA, *Ecosystems*, 12(1), 16–32, doi:10.1007/s10021-008-9201-9.
- 1012 Moteki, N., and Y. Kondo (2010), Dependence of Laser-Induced Incandescence on Physical Properties of  
1013 Black Carbon Aerosols: Measurements and Theoretical Interpretation, *Aerosol Sci. Technol.*, 44(8),  
1014 663–675, doi:10.1080/02786826.2010.484450.
- 1015 Moteki, N., Y. Kondo, Y. Miyazaki, N. Takegawa, Y. Komazaki, G. Kurata, T. Shirai, D. R. Blake, T.  
1016 Miyakawa, and M. Koike (2007), Evolution of mixing state of black carbon particles: Aircraft  
1017 measurements over the western Pacific in March 2004, *Geophys. Res. Lett.*, 34(11), L11803,  
1018 doi:10.1029/2006GL028943.
- 1019 Murphy, S. M. et al. (2009), Comprehensive Simultaneous Shipboard and Airborne Characterization of  
1020 Exhaust from a Modern Container Ship at Sea, *Environ. Sci. Technol.*, 43(13), 4626–4640,  
1021 doi:10.1021/es802413j.
- 1022 Ortega, A. M., D. A. Day, M. J. Cubison, W. H. Brune, D. Bon, J. A. de Gouw, and J. L. Jimenez (2013),  
1023 Secondary organic aerosol formation and primary organic aerosol oxidation from biomass-burning  
1024 smoke in a flow reactor during FLAME-3, *Atmos. Chem. Phys.*, 13(22), 11551–11571,  
1025 doi:10.5194/acp-13-11551-2013.
- 1026 Paris, J.-D., A. Stohl, P. Nédélec, M. Y. Arshinov, M. V. Panchenko, V. P. Shmargunov, K. S. Law, B. D.  
1027 Belan, and P. Ciais (2009), Wildfire smoke in the Siberian Arctic in summer: source  
1028 characterization and plume evolution from airborne measurements, *Atmos. Chem. Phys.*, 9(23),  
1029 9315–9327, doi:10.5194/acp-9-9315-2009.
- 1030 Park, R. J., D. J. Jacob, and J. A. Logan (2007), Fire and biofuel contributions to annual mean aerosol  
1031 mass concentrations in the United States, *Atmos. Environ.*, 41(35), 7389–7400,  
1032 doi:10.1016/j.atmosenv.2007.05.061.
- 1033 Petzold, A. et al. (2013), Recommendations for reporting “black carbon” measurements, *Atmos. Chem.*  
1034 *Phys.*, 13(16), 8365–8379, doi:10.5194/acp-13-8365-2013.
- 1035 Phuleria, H. C., P. M. Fine, Y. F. Zhu, and C. Sioutas (2005), Air quality impacts of the October 2003  
1036 Southern California wildfires, *J. Geophys. Res.*, 110(D7), D07S20, doi:10.1029/2004JD004626.

- 1037 Ramanathan, V., and G. Carmichael (2008), Global and regional climate changes due to black carbon,  
1038 *Nat. Geosci.*, *1*(4), 221–227, doi:10.1038/ngeo156.
- 1039 Reid, J. S., R. Koppmann, T. F. Eck, and D. P. Eleuterio (2005), A review of biomass burning emissions  
1040 part II: intensive physical properties of biomass burning particles, *Atmos. Chem. Phys.*, *5*(3), 799–  
1041 825, doi:10.5194/acp-5-799-2005.
- 1042 Robinson, A. L., N. M. Donahue, M. K. Shrivastava, E. A. Weitkamp, A. M. Sage, A. P. Grieshop, T. E.  
1043 Lane, J. R. Pierce, S. N. Pandis, and S. Emissions (2007), Rethinking organic aerosols: semivolatile  
1044 emissions and photochemical aging., *Science*, *315*(5816), 1259–62, doi:10.1126/science.1133061.
- 1045 Robinson, A. L., A. P. Grieshop, N. M. Donahue, and S. W. Hunt (2010), Updating the Conceptual  
1046 Model for Fine Particle Mass Emissions from Combustion Systems Allen L. Robinson, *J. Air Waste*  
1047 *Manage. Assoc.*, *60*(10), 1204–1222, doi:10.3155/1047-3289.60.10.1204.
- 1048 Sahu, L. K. et al. (2012), Emission characteristics of black carbon in anthropogenic and biomass burning  
1049 plumes over California during ARCTAS-CARB 2008, *J. Geophys. Res.*, *117*(D16), D16302,  
1050 doi:10.1029/2011JD017401.
- 1051 Saleh, R., C. J. Hennigan, G. R. McMeeking, W. K. Chuang, E. S. Robinson, H. Coe, N. M. Donahue,  
1052 and A. L. Robinson (2013), Absorptivity of brown carbon in fresh and photo-chemically aged  
1053 biomass-burning emissions, *Atmos. Chem. Phys.*, *13*(15), 7683–7693, doi:10.5194/acp-13-7683-  
1054 2013.
- 1055 Schwarz, J. P. et al. (2006), Single-particle measurements of midlatitude black carbon and light-scattering  
1056 aerosols from the boundary layer to the lower stratosphere, *J. Geophys. Res.*, *111*(D16), D16207,  
1057 doi:10.1029/2006JD007076.
- 1058 Schwarz, J. P. et al. (2008), Measurement of the mixing state, mass, and optical size of individual black  
1059 carbon particles in urban and biomass burning emissions, *Geophys. Res. Lett.*, *35*(13), L13810,  
1060 doi:10.1029/2008GL033968.
- 1061 Slowik, J. G. et al. (2007), An Inter-Comparison of Instruments Measuring Black Carbon Content of Soot  
1062 Particles, *Aerosol Sci. Technol.*, *41*(3), 295–314, doi:10.1080/02786820701197078.
- 1063 Sorooshian, A., S. M. Murphy, S. Hersey, R. Bahreini, H. Jonsson, R. C. Flagan, and J. H. Seinfeld  
1064 (2010), Constraining the contribution of organic acids and AMS m/z 44 to the organic aerosol  
1065 budget: On the importance of meteorology, aerosol hygroscopicity, and region, *Geophys. Res. Lett.*,  
1066 *37*(21), L21807, doi:10.1029/2010GL044951.
- 1067 Spackman, J. R., J. P. Schwarz, R. S. Gao, L. A. Watts, D. S. Thomson, D. W. Fahey, J. S. Holloway, J.  
1068 A. de Gouw, M. Trainer, and T. B. Ryerson (2008), Empirical correlations between black carbon  
1069 aerosol and carbon monoxide in the lower and middle troposphere, *Geophys. Res. Lett.*, *35*(19),  
1070 L19816, doi:10.1029/2008GL035237.
- 1071 Spracklen, D. V., L. J. Mickley, J. A. Logan, R. C. Hudman, R. Yevich, M. D. Flannigan, and A. L.  
1072 Westerling (2009), Impacts of climate change from 2000 to 2050 on wildfire activity and  
1073 carbonaceous aerosol concentrations in the western United States, *J. Geophys. Res.*, *114*(D20),  
1074 D20301, doi:10.1029/2008JD010966.

- 1075 Stephens, M., N. Turner, and J. Sandberg (2003), Particle Identification by Laser-Induced Incandescence  
1076 in a Solid-State Laser Cavity, *Appl. Opt.*, *42*(19), 3726, doi:10.1364/AO.42.003726.
- 1077 Subramanian, R., C. A. Roden, P. Boparai, and T. C. Bond (2007), Yellow Beads and Missing Particles:  
1078 Trouble Ahead for Filter-Based Absorption Measurements, *Aerosol Sci. Technol.*, *41*(6), 630–637,  
1079 doi:10.1080/02786820701344589.
- 1080 Subramanian, R. et al. (2010), Black carbon over Mexico: the effect of atmospheric transport on mixing  
1081 state, mass absorption cross-section, and BC/CO ratios, *Atmos. Chem. Phys.*, *10*(1), 219–237,  
1082 doi:10.5194/acp-10-219-2010.
- 1083 Sueper, D., P. F. DeCarlo, A. C. Aiken, and J. L. Jimenez (2013), ToF-AMS High Resolution Analysis  
1084 Software, Available from: [http://cires.colorado.edu/jimenez-group/wiki/index.php/ToF-](http://cires.colorado.edu/jimenez-group/wiki/index.php/ToF-AMS_Analysis_Software)  
1085 [AMS\\_Analysis\\_Software](http://cires.colorado.edu/jimenez-group/wiki/index.php/ToF-AMS_Analysis_Software)
- 1086 Sullivan, A. P., A. A. May, T. Lee, G. R. McMeeking, S. M. Kreidenweis, S. K. Akagi, R. J. Yokelson, S.  
1087 P. Urbanski, and J. L. Collett Jr. (2014), Airborne characterization of smoke marker ratios from  
1088 prescribed burning, *Atmos. Chem. Phys. Discuss.*, *14*(8), 11715–11747, doi:10.5194/acpd-14-11715-  
1089 2014.
- 1090 Turpin, B. B. J., and H.-J. H. Lim (2001), Species Contributions to PM<sub>2.5</sub> Mass Concentrations:  
1091 Revisiting Common Assumptions for Estimating Organic Mass, *Aerosol Sci. Technol.*, *35*(1), 602–  
1092 610, doi:10.1080/02786820119445.
- 1093 Urbanski, S. P. (2013), Combustion efficiency and emission factors for wildfire-season fires in mixed  
1094 conifer forests of the northern Rocky Mountains, US, *Atmos. Chem. Phys.*, *13*(14), 7241–7262,  
1095 doi:10.5194/acp-13-7241-2013.
- 1096 Ward, D. E., and C. C. Hardy (1991), Smoke emissions from wildland fires, *Environ. Int.*, *17*(2-3), 117–  
1097 134, doi:10.1016/0160-4120(91)90095-8.
- 1098 Watson, J. G., J. C. Chow, and L.-W. A. Chen (2005), Summary of Organic and Elemental Carbon/Black  
1099 Carbon Analysis Methods and Intercomparisons, *Aerosol Air Qual. Res.*, *5*(1), 65–102.
- 1100 Watson, J. G. J. et al. (2011), Particulate emission factors for mobile fossil fuel and biomass combustion  
1101 sources., *Sci. Total Environ.*, *409*(12), 2384–96, doi:10.1016/j.scitotenv.2011.02.041.
- 1102 Weimer, S., M. R. Alfarra, D. Schreiber, M. Mohr, A. S. H. Prévôt, and U. Baltensperger (2008), Organic  
1103 aerosol mass spectral signatures from wood-burning emissions: Influence of burning conditions and  
1104 wood type, *J. Geophys. Res.*, *113*(D10), D10304, doi:10.1029/2007JD009309.
- 1105 Van der Werf, G. R., J. T. Randerson, L. Giglio, G. J. Collatz, M. Mu, P. S. Kasibhatla, D. C. Morton, R.  
1106 S. DeFries, Y. Jin, and T. T. van Leeuwen (2010), Global fire emissions and the contribution of  
1107 deforestation, savanna, forest, agricultural, and peat fires (1997–2009), *Atmos. Chem. Phys.*, *10*(23),  
1108 11707–11735, doi:10.5194/acp-10-11707-2010.
- 1109 Westerling, A. L., H. G. Hidalgo, D. R. Cayan, and T. W. Swetnam (2006), Warming and earlier spring  
1110 increase western U.S. forest wildfire activity., *Science*, *313*(5789), 940–3,  
1111 doi:10.1126/science.1128834.

1112 Wiedinmyer, C., B. Quayle, C. Geron, A. Belote, D. McKenzie, X. Zhang, S. O'Neill, and K. K. Wynne  
1113 (2006), Estimating emissions from fires in North America for air quality modeling, *Atmos. Environ.*,  
1114 40(19), 3419–3432, doi:10.1016/j.atmosenv.2006.02.010.

1115 Wiedinmyer, C., S. K. Akagi, R. J. Yokelson, L. K. Emmons, J. A. Al-Saadi, J. J. Orlando, and A. J. Soja  
1116 (2011), The Fire INventory from NCAR (FINN): a high resolution global model to estimate the  
1117 emissions from open burning, *Geosci. Model Dev.*, 4(3), 625–641, doi:10.5194/gmd-4-625-2011.

1118 Yamasoe, M. A., P. Artaxo, A. H. Miguel, and A. G. Allen (2000), Chemical composition of aerosol  
1119 particles from direct emissions of vegetation fires in the Amazon Basin: water-soluble species and  
1120 trace elements, *Atmos. Environ.*, 34(10), 1641–1653, doi:10.1016/S1352-2310(99)00329-5.

1121 Yelverton, T. L. B., M. D. Hays, B. K. Gullett, and W. P. Linak (2014), Black Carbon Measurements of  
1122 Flame-Generated Soot as Determined by Optical, Thermal-Optical, Direct Absorption, and Laser  
1123 Incandescence Methods, *Environ. Eng. Sci.*, 31(4), 209–215, doi:10.1089/ees.2014.0038.

1124 Yokelson, R. J., D. W. T. Griffith, and D. E. Ward (1996), Open-path Fourier transform infrared studies  
1125 of large-scale laboratory biomass fires, *J. Geophys. Res.*, 101(D15), 21067, doi:10.1029/96JD01800.

1126 Yokelson, R. J., J. G. Goode, D. E. Ward, R. A. Susott, R. E. Babbitt, D. D. Wade, I. Bertschi, D. W. T.  
1127 Griffith, and W. M. Hao (1999), Emissions of formaldehyde, acetic acid, methanol, and other trace  
1128 gases from biomass fires in North Carolina measured by airborne Fourier transform infrared  
1129 spectroscopy, *J. Geophys. Res.*, 104(D23), 30109, doi:10.1029/1999JD900817.

1130 Yokelson, R. J. et al. (2007), Emissions from forest fires near Mexico City, *Atmos. Chem. Phys.*, 7(21),  
1131 5569–5584, doi:10.5194/acp-7-5569-2007.

1132 Yokelson, R. J. et al. (2009), Emissions from biomass burning in the Yucatan, *Atmos. Chem. Phys.*, 9(15),  
1133 5785–5812, doi:10.5194/acp-9-5785-2009.

1134 Yokelson, R. J. et al. (2013a), Coupling field and laboratory measurements to estimate the emission  
1135 factors of identified and unidentified trace gases for prescribed fires, *Atmos. Chem. Phys.*, 13(1), 89–  
1136 116, doi:10.5194/acp-13-89-2013.

1137 Yokelson, R. J., M. O. Andreae, and S. K. Akagi (2013b), Pitfalls with the use of enhancement ratios or  
1138 normalized excess mixing ratios measured in plumes to characterize pollution sources and aging,  
1139 *Atmos. Meas. Tech.*, 6(8), 2155–2158, doi:10.5194/amt-6-2155-2013.

1140 Yu, J. Z., J. Xu, and H. Yang (2002), Charring Characteristics of Atmospheric Organic Particulate Matter  
1141 in Thermal Analysis, *Environ. Sci. Technol.*, 36(4), 754–761, doi:10.1021/es015540q.

1142

1143

1144

1145 **Tables**

1146 Table 1. Summary of prescribed fires sampled during the SLOBB (CA) and SCREAM (SC) campaigns,  
 1147 compiled from previous studies [Burling *et al.*, 2011; Akagi *et al.*, 2013; Sullivan *et al.*, 2014]. Values for  
 1148 the area burned for the two Grant fires have been updated to reflect correct values.  
 1149

Fire name	Location	Date	Fuel description	Area burned (ha)	Latitude	Longitude
Shaver	Fresno, CA	10 Nov 2009	Conifer forest understory	30	37.0652	-119.2897
Turtle	Fresno, CA	10 Nov 2009	Sierra mixed conifer with shrub understory	1050	36.9670	-119.0803
Grant A	Vandenberg AFB, CA	11 Nov 2009	Coastal sage scrub/grass	55	34.7925	-120.5297
Grant B	Vandenberg AFB, CA	11 Nov 2009	Maritime chaparral/grass	53	34.7983	-120.5250
Williams	Buellton, CA	17 Nov 2009	Coastal/maritime chaparral	81	34.7003	-120.2083
Atmore	Ventura, CA	18 Nov 2009	Coastal scrub sage	10	34.3152	-119.2278
Fort Jackson 6	Columbia, SC	30 Oct 2011	Mature long leaf pine*	61.9	34.0247	-80.8711
Fort Jackson 9	Columbia, SC	1 Nov 2011	Mature long leaf pine, sparkleberry*	36	34.0041	-80.8769
Fort Jackson 22b	Columbia, SC	2 Nov 2011	Mature long leaf/loblolly pine and oak*	28.7	34.0845	-80.7731
Georgetown	Georgetown, SC	7 Nov 2011	Coastal grass understory	60.7	33.2025	-79.4016
Francis Marion	National Forest, SC	8 Nov 2011	Longleaf pine wiregrass	147	33.2153	-79.4761
Bamberg A	Bamberg, SC	10 Nov 2011	Longleaf/loblolly pine understory	36.4 <sup>#</sup>	33.2357 <sup>#</sup>	-80.9447 <sup>#</sup>
Bamberg B	Bamberg, SC	10 Nov 2011	Marsh grasses			

1150 \* Sullivan *et al.* [2014] also indicate that wiregrass (or similar grassy fuels) were consumed during these  
 1151 fires, based on smoke marker ratios.

1152 <sup>#</sup> The Bamberg fire was comprised of many small fires and was initially considered as one fire during the  
 1153 research flights. However, Sullivan *et al.* [2014] propose that this is fires from distinct biomass sources  
 1154 due to differences in spatiotemporal smoke marker ratios, which we have independently confirmed with  
 1155 AMS, SP2, and CRDS data.  
 1156

1157 Table 2. Types and characteristics of fuels burned during the FLAME-III laboratory experiments. Fuel  
 1158 carbon fraction and moisture contents are expressed as percentages of dry mass. Identification numbers  
 1159 refer to specific burns during FLAME-III.  
 1160

Common name	Scientific name	Ecosystem type	IDs	Carbon fraction (dry weight %)	Moisture content (dry weight %)	Initial fuel mass (g)
Alaskan duff	Multiple species	boreal	51	47.6	19.2	200
Black spruce	<i>Picea mariana</i>	boreal	39	53.7	10.9	250
Ceanothus	Ceanothus L.	chaparral	62	53.2	9.9	1002
Chamise	<i>Adenostoma fasciculatum</i>	chaparral	59	55.3	10.0	500
Gallberry	<i>Ilex glabra</i>	SE coastal plain	44	55.6	39.3	500
			47		63.3	500
			38		45.5	250
Lodgepole pine	<i>Pinus contorta</i>	montane	50	54.3	82.8	150
			61		60.7	203
			54		11.1	500
Manzanita	<i>Arctostaphylos</i> spp.	chaparral	60	54.3	8.4	502
Peat	multiple species	Indonesian peat	64	60.4	177.7	344
Pocosin	multiple species	palustrine wetland	41	54.5	9.1	400
			63		8.4	799
			40		74.2	250
Ponderosa pine	<i>Pinus ponderosa</i>	montane	48	55.4	84.2	200
			57		77.6	201
Sagebrush	<i>Artemisia tridentate</i>	sage scrubland	49	51.5	15.5	300
			53		15.6	300
Saw grass	<i>Cladium jamaicense</i>	Everglades	43	50.7	10.8	350
			58		8.0	525
Turkey oak	<i>Quercus laevis</i>	SE coastal plain	45	52.5	11.4	400
			52		42.8	401
Wheat straw	<i>Triticum</i> spp.	agricultural	46	47.1	9.0	500
White spruce	<i>Picea glauca</i>	boreal	55	52.9	9.0	346
Wire grass	<i>Aristida stricta</i>	SE coastal plain	42	50.9	29.4	600
			56		12.1	500

1161

1162

1163 Table 3. Emission ratios measured for aerosol components during individual laboratory burns and prescribed fires as well as averages by  
 1164 ecosystem types. Type indicates either laboratory measurements (L) or aircraft measurement (A). Numbers in parentheses indicate specific burn  
 1165 IDs in the case of repeated fuels during FLAME-III. Ecosystem averages are reported  $\pm$  one standard deviation. Units for rBC are presented based  
 1166 on standard convention; conversion to g rBC g-CO<sup>-1</sup> can be achieved via multiplication by a factor of 8.7x10<sup>-4</sup>. PM<sub>1</sub> refers to particulate matter  
 1167 with aerodynamic diameter less than 1  $\mu$ m as represented by the sum of rBC, OA, SO<sub>4</sub><sup>2-</sup>, NO<sub>3</sub><sup>-</sup>, NH<sub>4</sub><sup>+</sup>, and Chl<sup>-</sup>. Airborne MCE are based on FTIR  
 1168 measurements [Burling *et al.*, 2011; Akagi *et al.*, 2013], while laboratory MCE were calculated from gas analyzer measurements. Fuel moistures  
 1169 are repeated from Table 2. Also provided are fire-averaged (laboratory) and average plume-integrated (aircraft) OA mass concentrations (C<sub>OA</sub>).  
 1170

Fuel/fire	Type	MCE	Fuel moisture (dry wt. %)	rBC (ng sm <sup>-3</sup> ppbv <sup>-1</sup> )	OA (g g <sup>-1</sup> )	SO <sub>4</sub> <sup>2-</sup> (mg g <sup>-1</sup> )	NO <sub>3</sub> <sup>-</sup> (mg g <sup>-1</sup> )	NH <sub>4</sub> <sup>+</sup> (mg g <sup>-1</sup> )	Chl <sup>-</sup> (mg g <sup>-1</sup> )	PM <sub>1</sub> (g g <sup>-1</sup> )	C <sub>OA</sub> ( $\mu$ g sm <sup>-3</sup> ) <sup>§</sup>
<b>Chaparral</b>											
Ceanothus	L	0.942	9.9	-	0.048	3.0	0.8	0.1	1.7	-	945
Chamise	L	0.943	10.0	22.1	0.008	3.7	0.2	0.0	0.6	0.04	72
Manzanita (54)	L	0.956	11.1	25.2	0.015	1.0	0.4	0.1	1.4	0.04	120
Manzanita (60)	L	0.956	8.4	26.8	0.013	2.1	0.3	0.1	1.0	0.05	115
Atmore fire <sup>#</sup>	A	0.947	n/a	23.2	0.003	-	-	-	0.10	0.02	2.3
Grant A fire	A	0.938	n/a	27.9	0.033	0.19	0.59	0.36	1.7	0.06	88
Grant B fire	A	0.903	n/a	16.4	0.033	0.10	0.45	0.12	0.23	0.05	134
Williams fire	A	0.933	n/a	21.4	0.078	0.13	2.1	1.3	1.1	0.10	734
Laboratory average	L	0.949 $\pm$	9.9 $\pm$	24.7 $\pm$	0.021 $\pm$	2.5 $\pm$	0.4 $\pm$	0.07 $\pm$	1.2 $\pm$	0.043 $\pm$	313 $\pm$
		0.008	1.1	2.4	0.018	1.2	0.2	0.03	0.5 <sup>@</sup>	0.006	421
Aircraft average <sup>#</sup>	A	0.924 $\pm$	n/a	21.9 $\pm$	0.048 $\pm$	0.14 $\pm$	1.05 $\pm$	0.60 $\pm$	1.01 $\pm$	0.070 $\pm$	319 $\pm$
		0.019		5.8	0.026	0.04	0.92	0.63	0.74 <sup>@</sup>	0.026	360
<b>Montane</b>											
Lodgepole pine (38)	L	0.921	45.5	6.1	0.60	1.7	1.6	0.30	2.4	0.62	3160
Lodgepole pine (50)	L	0.889	82.8	2.0	1.24	2.1	5.6	0.66	1.0	1.25	3490
Lodgepole pine (61)	L	0.883	60.7	2.3	1.14	2.1	4.7	0.70	1.3	1.15	4980
Ponderosa pine (40)	L	0.889	74.2	1.5	1.53	1.5	2.9	0.59	0.7	1.53	6710
Ponderosa pine (48)	L	0.871	84.2	-	1.14	2.0	4.1	0.60	0.6	-	3620
Ponderosa pine (57)	L	0.892	77.6	2.1	1.19	1.9	4.7	0.78	0.7	1.20	5770
Shaver fire	A	0.885	n/a	6.7	0.104	0.07	1.7	0.48	0.13	0.11	174
Turtle fire	A	0.913	n/a	6.3	0.095	0.07	1.8	0.67	0.13	0.10	195
Laboratory average	L	0.891 $\pm$	70.8 $\pm$	2.8 $\pm$ 1.9	1.14 $\pm$	1.9 $\pm$	3.9 $\pm$	0.6 $\pm$	1.1 $\pm$	1.15 $\pm$	4620 $\pm$
		0.017	14.9		0.30	0.2	1.5	0.2	0.7 <sup>@</sup>	0.33	1430
Aircraft average	A	0.899 $\pm$ 0.020	n/a	6.5 $\pm$	0.10 $\pm$	0.07 $\pm$	1.7 $\pm$	0.58 $\pm$	0.13 $\pm$	0.11 $\pm$	185 $\pm$

Fuel/fire	Type	MCE	Fuel moisture (dry wt. %)	rBC (ng sm <sup>-3</sup> ppbv <sup>-1</sup> )	OA (g g <sup>-1</sup> )	SO <sub>4</sub> <sup>2-</sup> (mg g <sup>-1</sup> )	NO <sub>3</sub> <sup>-</sup> (mg g <sup>-1</sup> )	NH <sub>4</sub> <sup>+</sup> (mg g <sup>-1</sup> )	ChI <sup>-</sup> (mg g <sup>-1</sup> )	PM <sub>1</sub> (g g <sup>-1</sup> )	C <sub>OA</sub> (μg sm <sup>-3</sup> ) <sup>§</sup>
				0.3	0.01	0.001	0.06	0.13	0.001 <sup>@</sup>	0.01	15
<b>SE coastal plain</b>											
Gallberry (44)	L	0.954	39.3	18.0	0.19	2.9	1.0	0.1	1.3	0.21	1490
Gallberry (47)	L	0.947	63.3	18.9	0.29	1.7	1.2	0.1	0.9	0.31	1580
Pocosin (41)	L	0.960	9.1	21.5	0.03	0.7	0.3	0.1	0.7	0.05	168
Pocosin (63)	L	0.950	8.4	12.0	0.04	0.5	0.4	0.1	0.7	0.06	517
Turkey oak (45)	L	0.947	11.4	19.5	0.02	1.0	0.3	0.5	2.9	0.05	177
Turkey oak (52)	L	0.900	42.8	4.8	0.34	0.5	1.5	0.6	3.6	0.35	3770
Wire grass (42)	L	0.969	29.4	-	0.07	0.8	0.3	2.1	14.8	-	380
Wire grass (56)	L	0.959	12.1	16.0	0.20	0.8	1.3	1.4	11.1	0.23	869
FJ 6 fire	A	0.932	n/a	13.0	-	-	-	-	-	-	-
FJ 9a fire	A	0.919	n/a	8.2	0.026	1.00	0.43	0.37	0.14	0.035	904
FJ 22b fire	A	0.935	n/a	17.1	0.063	1.6	1.4	0.76	0.38	0.08	2200
Georgetown fire	A	0.938	n/a	21.8	0.028	1.3	1.5	1.5	5.4	0.06	266
Francis Marion fire	A	0.933	n/a	37.0	0.036	1.1	0.99	0.48	0.92	0.07	604
Bamberg A fire	A	0.943	n/a	16.7	0.047	4.5	2.0	1.6	0.53	0.07	393
Bamberg B fire	A	0.973	n/a	11.4	0.020	8.8	2.2	2.5	0.33	0.04	135
<i>Laboratory average</i>	<i>L</i>	<i>0.948 ± 0.021</i>	<i>27.0 ± 20.1</i>	<i>15.8 ± 5.7</i>	<i>0.15 ± 0.13</i>	<i>1.1 ± 0.8</i>	<i>0.8 ± 0.5</i>	<i>0.6 ± 0.8</i>	<i>4.5 ± 5.4<sup>@</sup></i>	<i>0.18 ± 0.13</i>	<i>1120 ± 1200</i>
<i>Aircraft average</i>	<i>A</i>	<i>0.936 ± 0.014</i>	<i>n/a</i>	<i>17.9 ± 9.5</i>	<i>0.037 ± 0.016</i>	<i>3.1 ± 3.1</i>	<i>1.4 ± 0.6</i>	<i>1.2 ± 0.8</i>	<i>1.3 ± 2.1<sup>@</sup></i>	<i>0.06 ± 0.02</i>	<i>750 ± 760</i>
<b>Boreal</b>											
Alaskan duff	L	0.900	19.2	0.5	0.12	0.3	0.8	0.2	0.1	0.12	832
Black spruce	L	0.957	10.9	19.3	0.07	0.4	0.4	0.1	1.0	0.10	233
White spruce	L	0.950	9.0	41.6	0.23	1.2	1.1	0.1	1.3	0.28	934
<i>Lab average</i>	<i>L</i>	<i>0.936 ± 0.031</i>	<i>13.0 ± 5.4</i>	<i>20.5 ± 20.6</i>	<i>0.14 ± 0.08</i>	<i>0.6 ± 0.5</i>	<i>0.8 ± 0.3</i>	<i>0.1 ± 0.1</i>	<i>0.8 ± 0.6<sup>@</sup></i>	<i>0.17 ± 0.10</i>	<i>666 ± 379</i>
<b>Others</b>											
Indonesian peat	L	0.891	177.7	0.03	0.20	0.4	0.8	0.4	0.4	0.20	1110
Sagebrush (49)*	L	0.925	15.5	20.0	0.02	8.2	0.7	0.1	3.4	0.05	154
Sagebrush (53)*	L	0.924	15.6	21.3	0.01	3.1	0.8	0.1	2.2	0.04	99
Saw grass (43)*	L	0.958	10.8	28.0	0.06	1.6	0.4	2.3	14.2	0.11	326
Saw grass (58)*	L	0.939	8.0	16.2	0.28	2.0	1.2	3.8	25.3	0.33	3044
Wheat straw	L	0.913	9.0	5.7	0.02	1.5	0.2	0.0	0.6	0.03	350

1171 \* Sagebrush and saw grass may sometimes be classified as chaparral and SE coastal plain fuels, respectively.

1172 # Atmore fire data excluded from average values, as described in the text.

1173 @ Average of  $PM_{10}$ , not sum of the average of the components. This value differs slightly from the sum of the averages due to the exclusion of  
1174 certain components that were unavailable (e.g., rBC for ponderosa pine with burn ID = 48)

1175 \$ Fire-averaged OA mass concentration for laboratory measurements, average plume-integrated OA mass concentration for aircraft measurements

1176

1177

1178

1179 Table 4. Emission factors measured for aerosol components during individual laboratory burns and prescribed fires as well as averages. Type  
 1180 indicates either laboratory measurements (L) or aircraft measurement (A). Aircraft measurements are restricted to values near the source and do  
 1181 not account for changes in the emission factor due to dilution. Numbers in parentheses indicate specific burn IDs in the case of repeated fuels  
 1182 during FLAME-III. Ecosystem averages are reported  $\pm$  one standard deviation. Units for all components are g kg-dry-fuel-consumed<sup>-1</sup>. PM<sub>1</sub> refers  
 1183 to particulate matter with aerodynamic diameter less than 1  $\mu$ m as represented by the sum of rBC, OA, SO<sub>4</sub><sup>2-</sup>, NO<sub>3</sub><sup>-</sup>, NH<sub>4</sub><sup>+</sup>, and Chl<sup>-</sup>. Fuel moisture  
 1184 is repeated from Table 2 while MCE and C<sub>OA</sub> are repeated from Table 3.  
 1185

Fire/fuel	Type	MCE	Fuel moisture (dry wt. %)	rBC	OA	SO <sub>4</sub> <sup>2-</sup>	NO <sub>3</sub> <sup>-</sup>	NH <sub>4</sub> <sup>+</sup>	Chl <sup>-</sup>	PM <sub>1</sub>	C <sub>OA</sub> ( $\mu$ g sm <sup>-3</sup> ) <sup>s</sup>
<b>Chaparral</b>											
Ceanothus	L	0.942	9.9	-	3.4	0.22	0.05	0.00	0.12	-	945
Chamise	L	0.943	10.0	1.73	0.6	0.28	0.02	0.00	0.05	2.7	72
Manzanita (54)	L	0.956	11.1	1.49	0.8	0.06	0.02	0.00	0.08	2.5	120
Manzanita (60)	L	0.956	8.4	1.59	0.7	0.11	0.02	0.01	0.05	2.5	115
Atmore fire <sup>#</sup>	A	0.947	n/a	1.13	0.2	-	-	-	0.01	1.3	2.3
Grant A fire	A	0.938	n/a	1.56	2.3	0.01	0.04	0.03	0.12	4.1	88
Grant B fire	A	0.903	n/a	1.43	3.6	0.01	0.05	0.01	0.03	5.1	134
Williams fire	A	0.933	n/a	1.30	5.9	0.01	0.16	0.10	0.08	7.4	734
<i>Laboratory average</i>	L	0.949 $\pm$	9.9 $\pm$	1.60 $\pm$	1.4 $\pm$	0.17 $\pm$	0.03 $\pm$	0.00 $\pm$	0.07 $\pm$	2.6 $\pm$	313 $\pm$
		0.008	1.1	0.12	1.3	0.10	0.02	0.00	0.03	0.1 <sup>@</sup>	421
<i>Aircraft average<sup>#</sup></i>	A	0.925 $\pm$	n/a	1.43 $\pm$	3.9 $\pm$	0.01 $\pm$	0.08 $\pm$	0.05 $\pm$	0.08 $\pm$	5.5 $\pm$	319 $\pm$
		0.019		0.13	1.8	0.01	0.07	0.05	0.05	1.7	360
<b>Montane</b>											
Lodgepole pine (38)	L	0.921	45.5	0.65	65.3	0.18	0.17	0.03	0.26	66.5	3160
Lodgepole pine (50)	L	0.889	82.8	0.30	184.4	0.25	0.67	0.09	0.14	185.9	3490
Lodgepole pine (61)	L	0.883	60.7	0.36	168.9	0.31	0.70	0.10	0.19	170.5	4980
Ponderosa pine (40)	L	0.889	74.2	0.22	218.1	0.21	0.41	0.08	0.10	219.1	6710
Ponderosa pine (48)	L	0.871	84.2	-	189.4	0.34	0.69	0.10	0.10	-	3620
Ponderosa pine (57)	L	0.892	77.6	0.31	191.9	0.30	0.76	0.11	0.11	193.5	5770
Shaver fire	A	0.885	n/a	0.68	13.2	0.01	0.2	0.06	0.02	14.1	174
Turtle fire	A	0.913	n/a	0.49	9.3	0.01	0.2	0.07	0.01	10.0	195
<i>Laboratory average</i>	L	0.891 $\pm$	70.8 $\pm$	0.37 $\pm$	169.7 $\pm$	0.26 $\pm$	0.57 $\pm$	0.09 $\pm$	0.15 $\pm$	167.1 $\pm$	4620 $\pm$
		0.017	14.9	0.16	53.6	0.06	0.23	0.03	0.06	58.9 <sup>@</sup>	1430
<i>Aircraft average</i>	A	0.899 $\pm$	n/a	0.59 $\pm$	11.2 $\pm$	0.008 $\pm$	0.2 $\pm$	0.06 $\pm$	0.01 $\pm$	12.1 $\pm$	185 $\pm$
		0.020		0.13	2.7	0.00	0.03	0.00	0.00	2.9	15
<b>SE coastal plain</b>											

Fire/fuel	Type	MCE	Fuel moisture (dry wt. %)	rBC	OA	SO <sub>4</sub> <sup>2-</sup>	NO <sub>3</sub> <sup>-</sup>	NH <sub>4</sub> <sup>+</sup>	Cl <sup>-</sup>	PM <sub>1</sub>	C <sub>OA</sub> (μg sm <sup>-3</sup> ) <sup>§</sup>
Gallberry (44)	L	0.954	39.3	1.13	11.2	0.18	0.06	0.01	0.08	12.7	1490
Gallberry (47)	L	0.947	63.3	1.37	21.1	0.13	0.09	0.01	0.06	22.7	1580
Pocosin (41)	L	0.960	9.1	1.17	1.5	0.04	0.02	0.00	0.04	2.8	168
Pocosin (63)	L	0.950	8.4	0.82	2.8	0.03	0.02	0.01	0.05	3.7	517
Turkey oak (45)	L	0.947	11.4	1.33	1.6	0.07	0.02	0.03	0.21	3.2	177
Turkey oak (52)	L	0.900	42.8	0.62	41.3	0.06	0.18	0.08	0.44	42.7	3770
Wire grass (42)	L	0.969	29.4	-	2.9	0.04	0.01	0.09	0.63	-	380
Wire grass (56)	L	0.959	12.1	0.83	9.6	0.04	0.06	0.07	0.54	11.1	869
FJ 6 fire	A	0.932	n/a	0.81	-	-	-	-	-	-	-
FJ 9a fire	A	0.919	n/a	0.68	2.54	0.10	0.04	0.04	0.01	3.42	904
FJ 22b fire	A	0.935	n/a	1.29	5.66	0.15	0.12	0.07	0.03	7.32	2200
Georgetown fire	A	0.938	n/a	1.36	2.09	0.09	0.11	0.11	0.40	4.16	266
Francis Marion fire	A	0.933	n/a	2.40	2.82	0.09	0.08	0.04	0.07	5.49	604
Bamberg A fire	A	0.943	n/a	0.94	3.12	0.30	0.13	0.10	0.04	4.63	393
Bamberg B fire	A	0.973	n/a	0.31	0.64	0.28	0.07	0.08	0.01	1.40	135
<i>Laboratory average</i>	L	0.948 ± 0.021	27.0 ± 20.1	1.04 ± 0.29	11.5 ± 13.8	0.07 ± 0.05	0.06 ± 0.05	0.04 ± 0.04	0.26 ± 0.24	14.1 ± 14.5 <sup>@</sup>	1120 ± 1200
<i>Aircraft average</i>	A	0.936 ± 0.014	n/a	1.11 ± 0.67	2.8 ± 1.6	0.17 ± 0.10	0.09 ± 0.03	0.07 ± 0.03	0.09 ± 0.15	4.4 ± 2.0	750 ± 760
<b>Boreal</b>											
Alaskan duff	L	0.900	19.2	0.06	27.5	0.06	0.17	0.05	0.03	27.9	832
Black spruce	L	0.957	10.9	1.11	4.1	0.02	0.02	0.01	0.05	5.3	233
White spruce	L	0.950	9.0	2.72	14.3	0.08	0.07	0.00	0.08	17.3	934
<i>Laboratory average</i>	L	0.936 ± 0.031	13.0 ± 5.4	1.29 ± 1.34	15.3 ± 11.7	0.05 ± 0.03	0.09 ± 0.08	0.02 ± 0.02	0.06 ± 0.02	16.8 ± 11.3 <sup>@</sup>	666 ± 379
<b>Others</b>											
Indonesian peat	L	0.891	177.7	0.01	34.5	0.07	0.16	0.07	0.07	34.9	1110
Sagebrush (49)*	L	0.925	15.5	2.02	1.7	0.74	0.06	0.01	0.30	4.9	154
Sagebrush (53)*	L	0.924	15.6	2.12	1.1	0.28	0.07	0.01	0.20	3.8	99
Saw grass (43)*	L	0.958	10.8	1.70	2.9	0.08	0.02	0.12	0.73	5.6	326
Saw grass (58)*	L	0.939	8.0	1.38	20.3	0.14	0.08	0.28	1.81	24.0	3044
Wheat straw	L	0.913	9.0	0.74	2.1	0.14	0.02	0.00	0.05	3.0	350

1186 \* Sagebrush and saw grass may sometimes be classified as chaparral and SE coastal plain fuels, respectively.

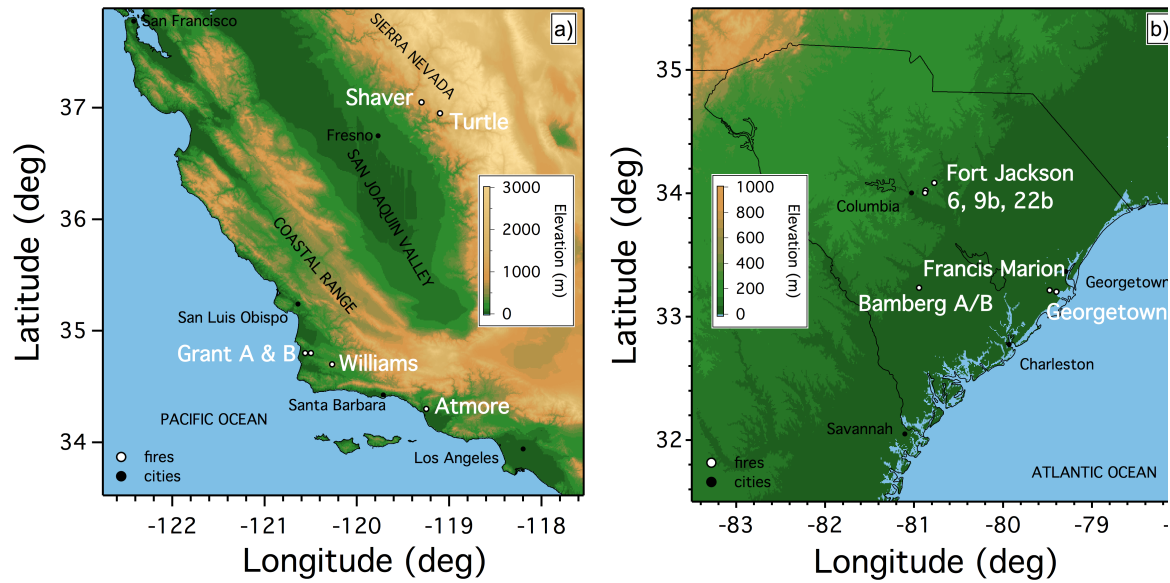
1187 # Atmore fire data excluded from average values, as described in the text.

1188 @ Average of  $PM_{10}$ , not sum of the average of the components. This value differs slightly from the sum of the averages due to the exclusion of  
1189 certain components that were unavailable (e.g., rBC for ponderosa pine with burn ID = 48)

1190 \$ Fire-averaged OA mass concentration for laboratory measurements, average plume-integrated OA mass concentration for aircraft measurements

1191

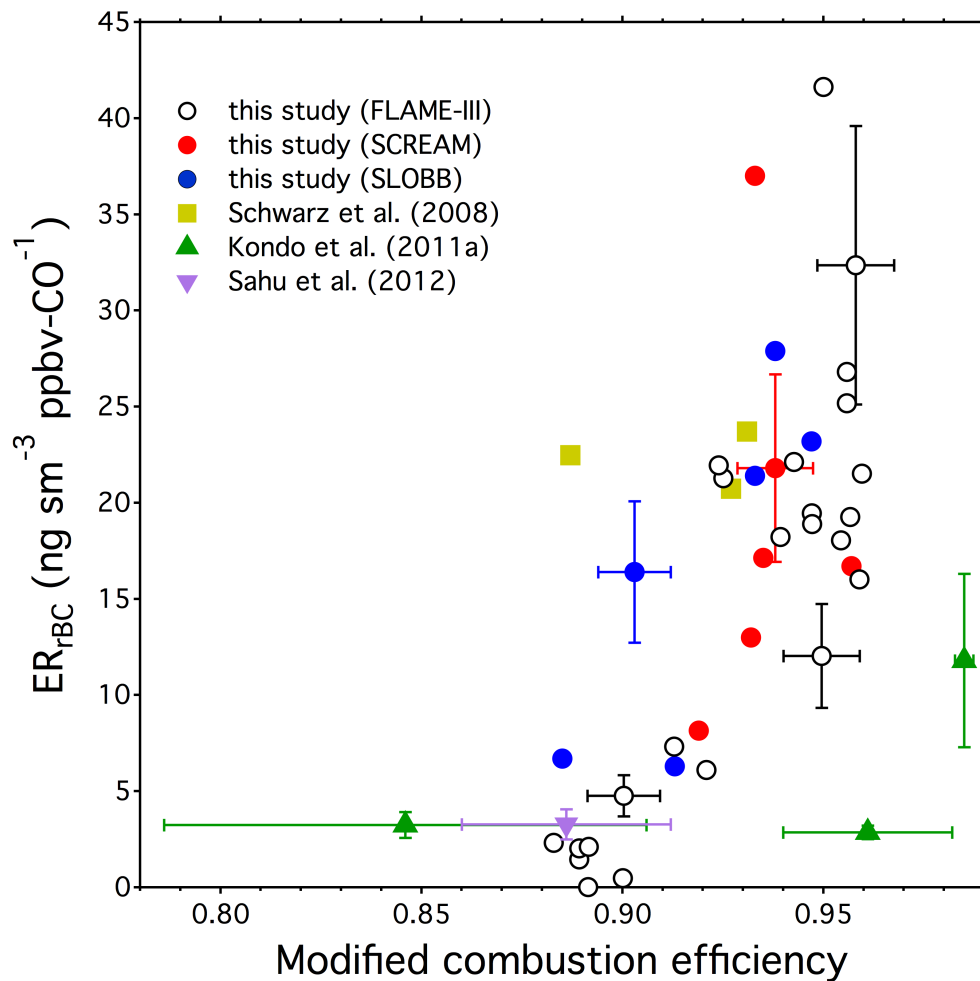
1192 **Figures**



1193

1194 Figure 1. Topographic maps of **a)** central California (SLOBB) and **b)** South Carolina (SCR)  
1195 showing locations of cities, prescribed fires and major geographical features. Note the differer  
1196 elevation scales between the two panels. More details on fire location, area burned, and fuels con  
1197 are provided in Table 1.

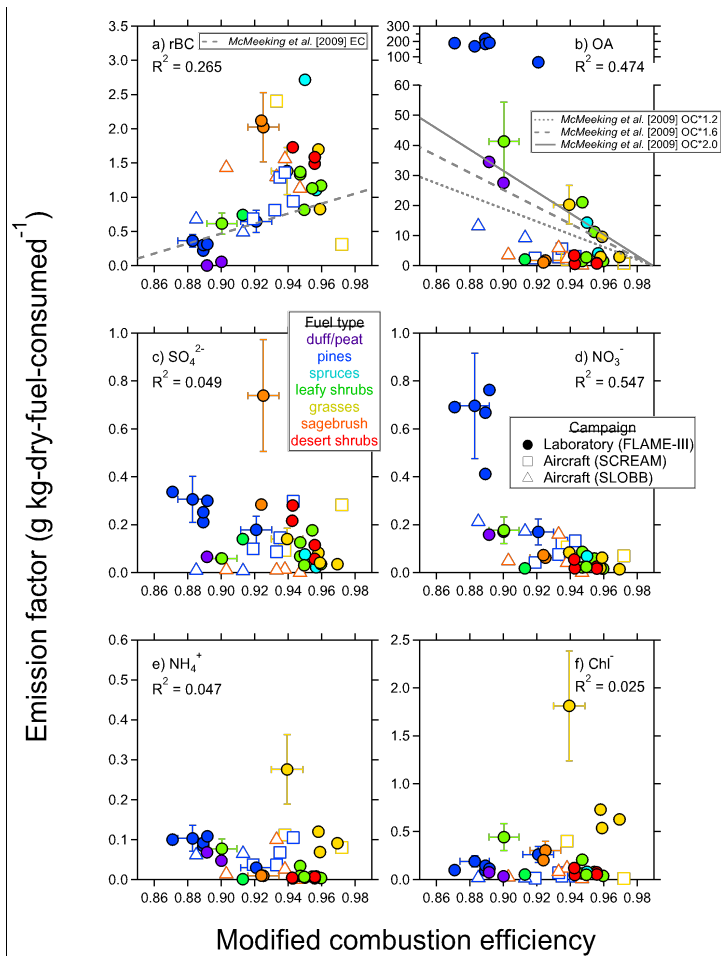
1198



1199

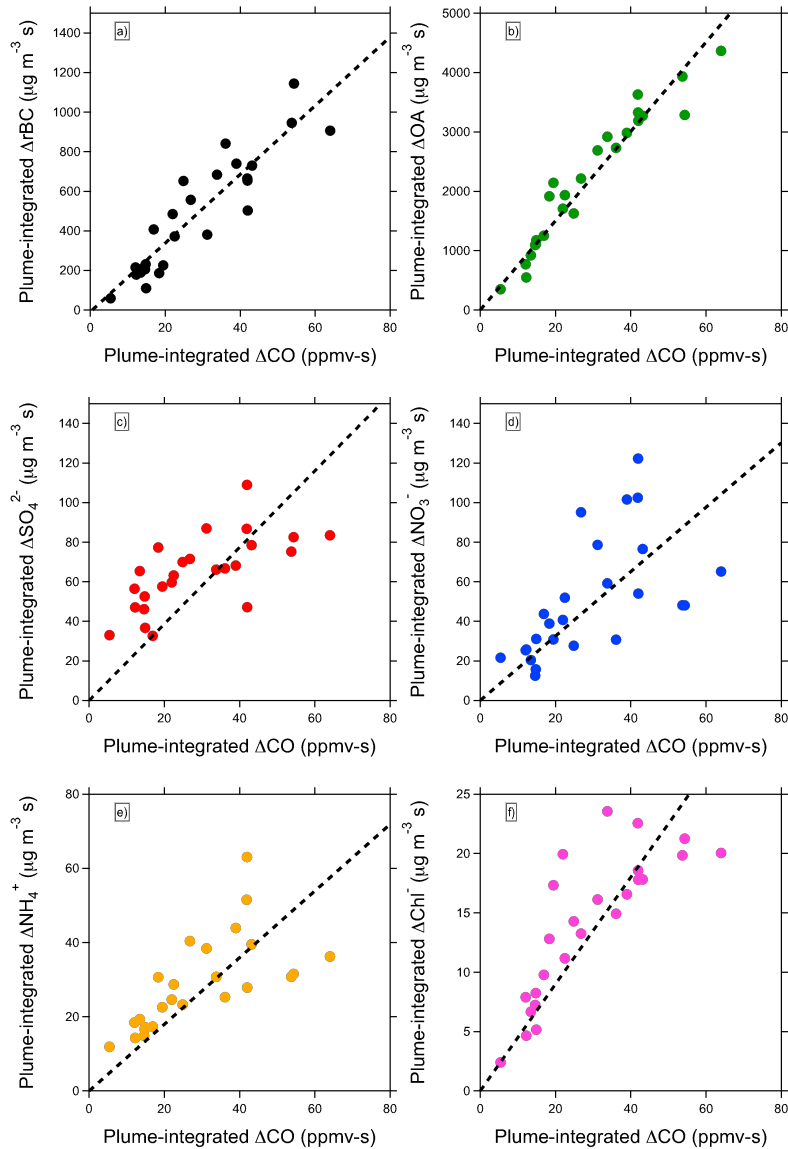
1200 Figure 2. Fire-averaged rBC emission ratios as a function of modified combustion efficiency for the  
 1201 FLAME-III laboratory burns and for aircraft measurements over prescribed fires. Representative  
 1202 measurement uncertainties of  $\pm 25\%$  in rBC measurements, 2% in CO measurements, and 1% in CO<sub>2</sub>  
 1203 measurements are propagated and shown for select data from our study. Published data for biomass  
 1204 burning plumes of varying atmospheric ages from Schwarz et al. [2008], Kondo et al. [2011b] and Sahu  
 1205 et al. [2012] are shown for comparison; uncertainty bars represent one standard deviation, where  
 1206 available, for these data.

1207



1208

1209 Figure 3. Emission factors measured for a) refractory black carbon (rBC) compared to EC from  
 1210 *McMeeking et al.* [2009], b) organic aerosol (OA) compared to the fit for OC from *McMeeking et al.*  
 1211 [2009] multiplied by factors of 1.2, 1.6, and 2.0 (see text for details), c) nitrate (NO<sub>3</sub><sup>-</sup>), d) sulfate (SO<sub>4</sub><sup>2-</sup>),  
 1212 e) ammonium (NH<sub>4</sub><sup>+</sup>) and f) chloride (Cl<sup>-</sup>) in the laboratory (FLAME-III) and over prescribed fires by  
 1213 aircraft during the SLOBB (CA) and SCREAM (SC) campaigns. Points are colored according to  
 1214 approximate fuel classification. Representative measurement uncertainties of ±30% in AMS  
 1215 measurements, ±25% in rBC measurements, 2% in CO measurements and 1% in CO<sub>2</sub> measurements are  
 1216 propagated and provided for select data from this study. Coefficients of determination derived from  
 1217 global linear regressions of each species are also provided.  
 1218

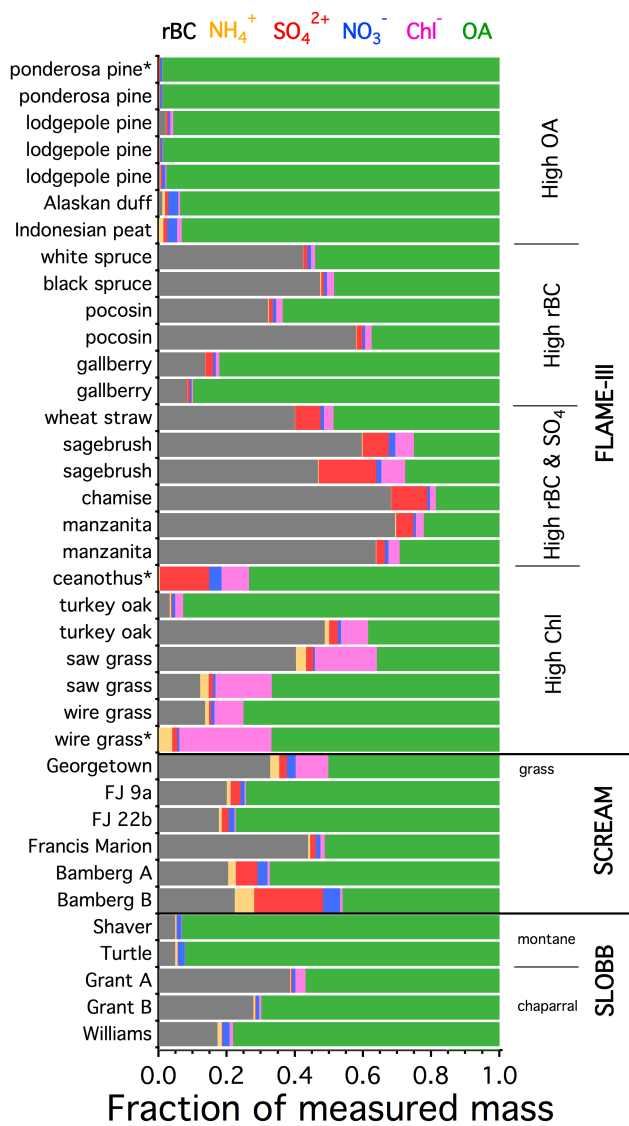


1219

1220

1221 Figure 4. Relationships between excess plume-integrated constituents of PM<sub>1</sub> based on SP2 and AMS  
 1222 measurements and excess CO from the CRDS for a)  $\Delta rBC$ , b)  $\Delta OA$ , c)  $\Delta NO_3^-$ , d)  $\Delta SO_4^{2-}$ , e)  $\Delta NH_4^+$ , and  
 1223 f)  $\Delta Chl^-$  for the Fort Jackson 22b fire on 2 November 2011. Lines show the regression of each species  
 1224 against  $\Delta CO$ . Each point represents a single plume intercept within 5 km of the source. Uncertainties in  
 1225 these measurements (not shown) are the same as described in Figure 3.

1226



1227  
 1228 Figure 5. Mass fractions of major species measured in sub-micron aerosol for laboratory and aircraft  
 1229 measurements. Fuels with (\*) do not include rBC in mass fraction calculations due to lack of data. The  
 1230 campaign during which the data were collected is provided to the right of the bars. Note that the mass  
 1231 fractions of OA for the pine species studied in the laboratory may be biased high due to high fuel  
 1232 moisture contents.  
 1233

1234

1235

1236